Supplementary information

For the article “Engineering genetic circuit interactions within and between synthetic minimal cells”

by Katarzyna P. Adamala, Daniel A. Martin-Alarcon, Katriona R. Guthrie-Honea, Edward S. Boyden

Supplementary Methods

Sources of materials and product characterization

The vectors used in this work were synthesized in house, from oligonucleotide gBlocks from IDT (IDT DNA, Coralville, IA, US) or DNA oligo building blocks from Epoch (Epoch Life Science Inc., Sugar Land, TX, US). The sequence of all plasmids was confirmed by Sanger Sequencing by Eton Bioscience Inc. (San Diego, CA, US) or Quintara Bio (Boston, MA, US). Unless otherwise stated, small molecules, activators and buffer components, were purchased either form Sigma Aldrich (St. Louis, MO, US) or Thermo Fisher (Waltham, MA, US) and were used without further purification. All antibiotics used for cloning and TL/TL preparation were purchased from GoldBio (Olivette, MO, US) and used without further purification. All experiments were performed in buffers prepared using RNAse free water from Ambion (sold by Thermo Fisher). The lipids used fo liposome formation were purchased from Avanti Polar Lipids (Alabaster, AL, US) and were used without further purification.

The enzyme products obtained in cell-free reactions were characterized with commercially available detection kits: Renilla, NanoLuc and Firefly luciferases using products from Promega (Madison, WI, US); Beta-lactamase, Chloramphenicol acetyltransferase and Beta-galactosidase using product from Thermo Fisher (Waltham, MA, US).

Liposome preparation

Our procedure for preparing liposomes was based on previously published protocols, most notably with the specific modifications described by the Mansy Lab[11,48]. Briefly, a chloroform solution of 20 mg (26 µmol) of POPC (Avanti Polar Lipids) and 20 mg (52 µmol) of cholesterol (Avanti Polar Lipids) was evaporated into a thin film using a round bottom flask. 4 mL of DEPC-treated nuclease-free water was added to the flask and vigorously vortexed for ~3 minutes. The liposome solution (~6.5 mM) was then homogenized with a hand-held homogenizer (IKA) for ~1 minute. The mixture was divided into 150 µL aliquots (~1 µmol of lipid each) and lyophilized until dry.

To prepare the final experimental liposome solution, aliquots of lyophilized lipids were hydrated with buffer containing the cell-free TX/TL extract, DNA, and small molecule activators for each experiment, to the final volume of 50 µL per reaction (~20 mM liposomes). Liposomes were extruded through a 1 µM polycarbonate track-etched membrane (Whatman). The unencapsulated solutes were removed from liposomes through dialysis using a liposome dialyzer as described previously[49], with a 0.5 mL volume slide-a-lyzer chamber and a 0.4 µM pore size polycarbonate track-etched membrane (Whatman). The dialysis was performed at 4°C. The samples were dialyzed 5 times against Dialysis Buffer (50 mM HEPES, pH=7.6, 100 mM KCl, 10 mM $MgCl_2$ and ~10mM empty and unlabeled POPC-cholesterol liposomes), with a buffer change every 10 minutes and 3 additional buffer changes every 20 minutes.

Renilla luciferase assays

Renilla luciferase (rLuc) activity was assayed using the Renilla Luciferase Assay System (Promega). Liposome reactions were stopped using Quench Mix according to the procedure described in section "Firefly luciferase assays" of **Materials and Methods**. The resulting sample was used directly with the Renilla luciferase assay, according to the manufacturer's instructions. The result is given in RLU—relative light units with 10 s integration time.

NanoLuc luciferase assays

NanoLuc luciferase activity was assayed using the Nano-Glo Luciferase Assay System (Promega). Liposome reactions were stopped using Quench Mix according to the procedure described in section "Firefly luciferase assays" of Materials and Methods. The resulting sample was used directly with the Nano-Glo luciferase assay, according to the manufacturer's instructions.

Beta-lactamase assays

Beta-lactamase activity was assayed using the LyticBLAzer-FRET B/G assay kit (Thermo). Liposome reactions were stopped using Quench Mix according to the procedure described in section "Firefly luciferase assays" of Materials and Methods. The resulting sample was used directly with the beta-lactamase assay, according to the manufacturer's instructions.

Beta-galactosidase assays

Beta-galactosidase activity was assayed using the β-Gal Assay Kit (Thermo). Liposome reactions were stopped using Quench Mix according to the procedure described in section "Firefly luciferase assays" of **Materials and Methods**. The resulting sample was used directly with the beta-galactosidase assay, according to the manufacturer's instructions.

Chloramphenicol acetyltransferase assays

Chloramphenicol acetyltransferase activity was assayed using the FAST CAT Green (Deoxy) Chloramphenicol Acetyltransferase Assay Kit (Thermo). Liposome reactions were stopped using Quench Mix according to the procedure described in section "Firefly luciferase assays" of **Materials and Methods**. Samples were then heated to 65°C for 10 minutes, to inactivate endogenous acetylating enzymes[1]. The resulting samples were used directly with the FAST CAT assay according to the manufacturer's instructions. GR ACS Silica Gel Grade 12 28-200 Mesh plates (EMD Millipore) were used for product analysis. After visualization, the product and substrate spots were scraped from the plate and mixed with 0.35 mL of methanol per spot. The samples were centrifuged for 1 min, a 200 µL aliquot of each methanol solution was removed, and the fluorescence of both substrate and product was quantified (excitation 490 mm, emission 525 mm).

Supplementary Discussion

Nomenclature

We use “liposomes”, “synells”, and “synthetic minimal cells” interchangeably throughout this paper. There is no universally acknowledged definition of synthetic minimal cells in the literature[2–6]. We understand synells as liposome bioreactors performing some of the biochemical functions of the living cell, most notably transcription and translation for the expression of proteins.

Expression of enzymatic reporter proteins in synthetic minimal cells

We focused on enzymatic reporters to measure protein expression in all our experiments, for these reporters can be quantitatively detected at very low concentrations, and with linear ranges that extend over several orders of magnitude[7–9]. We expressed firefly luciferase (fLuc), Renilla luciferase (rLuc), Nano-Luc luciferase[10], beta lactamase, beta galactosidase, and chloramphenicol acetyltransferase in liposomes, using the constitutively active P70 bacterial promoter (**Fig S3**). We assayed their enzymatic activity as a proxy for protein concentration, using multiple batch reactions run in parallel and collected at different time points. All five enzymatic reporters expressed well in synells.

The full list of all tested enzymatic reporter proteins, corresponding small molecule substrates, and expression profiles in cell-free bacterial system under T7 promoter is shown in **Fig. S3**. In addition to the luciferase activity luminescence assays, the identity of expressed firefly luciferase protein was confirmed using Western Blot analysis, **Fig. S4**.

Optimization of sequences for the theophylline riboswitch

It has been previously noted that putative ribosome binding sites (RBSs) inside the gene of interest might bypass the theophylline aptamer, resulting in expression of truncated genes independently of the theophylline riboswitch activity[11]. We screened the sequence of [P70][Theo][T7RNAP] for putative ribosome binding sites, using the sequence composition and spacing rules elucidated by Lentini et al[12]. Using the [T7][fLuc] reporter, we validated that T7RNAP expression is indeed under the control of the

theophylline riboswitch—with an amount of "leakage" comparable to previously reported levels[11] (see **Fig. S13b**).

Encapsulation efficiency and size distribution

The efficiency of solute encapsulation inside POPC liposomes of a given radius r (nm) at a given concentration c (mM) can be estimated using this formula, used in the Szostak Laboratory and empirically confirmed by encapsulation experiments :

%internal volume = vol_liposome*liposomes_ml*10^-19

Where:

vol_liposome = (4/3)*Pi*(r^3)

is the volume of the lumen of a single liposome, in nm^3;

liposomes_ml = surface_area_ml/area_liposome

is the number of liposomes per 1 mL;

surface_area_ml = (c*10^-6)*((760*10^21)/0.9*N_A)/2.5)/2

is the surface area of liposomes per 1 mL of solution of a given c (mM), with POPC MW=760 and length of the lipid bilayer approximated to 2.5nm; N_A is Avogadro's number;

and finally,

area_liposome = 4*Pi*(r^2)

is the surface area of the liposome outer leaflet, in nm^2.

These calculations were made with the assumption that liposome curvature is negligible, so the inner and outer leaflet contain an equal number of lipids and have equal surface area. The thickness of the bilayer was approximated at 2.5 nm[13]. The addition of cholesterol increases bilayer thickness up to 30%, thus affecting the encapsulation rate[14], but we cannot reliably estimate the influence of cholesterol on packing density and surface area of the liposomes. According to this formula, a 25 mM solution of 200 nm POPC liposomes will contain ~14% of the total volume encapsulated inside liposomes. In reality, the encapsulation rate of liposomes used in our experiments is likely lower. This is due to factors like the presence of cholesterol in POPC membranes and the fact, that in liposomes extruded through, e.g., a 200 nm filter, the size distribution of liposomes varies greatly and is, on average, smaller than 200nm[15–17]. The differences in yield of protein synthesis inside synthetic cells, explained by the difference in efficiency of encapsulating the TX/TL enzyme mix, have been observed before.[18]

We used DLS to analyze samples of liposomes prepared according to the protocol used in this work (see **Materials and Methods** and **Fig. S1**). The liposome sample size distribution is consistent between different preparations (samples from separate encapsulation, extrusion and dialysis processes, prepared on different days, are compared). The DLS experiments are very sensitive to fluorescent dyes present in the solution; therefore, we chose to perform those experiments on samples not producing any fluorescent reporter protein.

Efficiency of small molecule activator transfer

To assess the efficiency of IPTG activation between liposomes, we estimated the release of small molecules from liposomes through aHL channels. We prepared a sample of IPTG sensor liposomes like in experiments in **Fig. 5c**, but also containing 100 mM calcein—a fluorescent, non-membrane-permeable, small-molecule dye. Thus, the sensor liposomes contained both small molecules (IPTG and calcein) and the arabinose-inducible gene for aHL. We mixed these sensor liposomes 1:1 with reporter liposomes like those from **Fig. 5c** and incubated the mixture with arabinose. After incubation, we measured luciferase activity from half the liposome mixture and purified the other half on a Sepharose 4B size exclusion column, measuring the total fluorescence of the collected unencapsulated fraction. The concentration of the unencapsulated calcein, calculated from the dye fluorescence, was 0.18 mM in the 2.1 ml of the free dye fraction collected from the purification column. This corresponds to a concentration of ~3.78 mM in the original 100 µL sample of mixed liposomes; this can serve as an estimate of the concentration of small molecules that easily and maximally permeate through the aHL

pore (e.g., of IPTG). For reference, the initial concentration of IPTG and calcein in the liposome encapsulation mixture was 100 mM.

We performed an additional validation of this estimate for equilibrium IPTG concentration in the sensor-reporter mixture. We prepared a sample of reporter liposomes identical to those from **Fig. 5c**, and mixed it with empty liposomes plus IPTG to the final concentration of 3.78 mM. From this mixture we recorded a final luciferase activity of 28868 RLU (average of 3 samples, S. E. M. 815 RLU), which is comparable to the 20820 RLU recorded for the 1:1 mix of sensor and reporter liposomes in **Fig. 5c**.

We have further confirmed the insertion of the alpha hemolysin channel into the bilayer membrane of liposomes by two separate experiments. For the first experiment, we prepared the aHL as a fusion to the fluorescent protein mClover. We expressed the mClover-aHL fusion in large unilamellar vesicles prepared with Lissamine Rhodamine B (red fluorescent dye tethered to a phospholipid: 1,2-Dihexadecanoyl-sn-Glycero-3-Phosphoethanolamine, Triethylammonium Salt) in the phospholipid membrane. Direct confocal microscopy observation confirmed the co-localization of the green signal from the alpha hemolysin protein fusion with the red signal from the lipid-bound membrane dye (**Fig. S26**). For the second experiment, we prepared liposomes (as described in **Materials and Methods**) with two membrane dyes capable of FRET (Fluorescence Resonance Energy Transfer): Lissamine™ Rhodamine B 1,2-Dihexadecanoyl-sn-Glycero-3-Phosphoethanolamine, Triethylammonium Salt and NBD-PE N-(7-Nitrobenz-2-Oxa-1,3-Diazol-4-yl)-1,2-Dihexadecanoyl-sn-Glycero-3-Phosphoethanolamine, Triethylammonium Salt. Alpha hemolysin protein was expressed inside liposomes, from a constitutive bacterial P70 promoter, using bacterial TX/TL extract. The decrease in the observed FRET signal (increase in donor fluorescence and decrease in receptor fluorescence) indicated changes in the surface area of the liposome. This technique has been previously used to see insertion of biomolecules into the bilayer membrane of liposomes[19]. The observed increase of the membrane surface area is attributed to the insertion of the membrane protein into the bilayer. The negative control experiment, expressing firefly luciferase—a soluble protein with no known association to phospholipid membranes, results in no change of FRET signal over time.

Cascaded circuits

Cascaded circuits, in which the product of one gene triggers the production of the next, are useful for a variety of reasons—for signal amplification (i.e., a relatively small input signal can trigger a high

output), for modularity (e.g., a variety of sensors can be connected to a given output), and to enable multi-node control at various points within the network (as in the configuration of natural signaling and metabolic pathways in cells, where many reagents must be regulated in timing and concentration, for efficient synthesis). Such cascaded circuits are widely employed in synthetic circuits for these reasons[20,21]. We built cascaded circuits in this experiment using liposomes with *E. coli* TX/TL extract. The circuit we constructed had the gene for fLuc (in single component form) under a T7 promoter (recognized by T7 RNA Polymerase, T7RNAP), with the gene for T7RNAP itself under the control of a membrane-permeable activator (**Fig. S13a**), here either theophylline (Theo, which activates an aptamer sequence in the 5'-UTR that un-masks a ribosome binding site and triggers protein production) or arabinose (Ara, which induces the PBAD promoter). These activators had been previously tested in phospholipid liposomes for the induction of single genes[11,22].

We found the theophylline system to be leaky, as others have observed before[11] (expression for all time points after t = 3 h was significantly different from that at t = 0, $P < 0.0001$ in Sidak's multiple comparison test, after ANOVA with factors of time and presence or absence of theophylline; **Figs. S13b** and **S13c**; see **Table S9** for full statistics). We found no measurable activation of PBAD in the absence of arabinose, suggesting that arabinose may be a useful external trigger for cascaded genetic circuits (expression for all time points was equal to that for t = 0, $P > 0.9999$ in Sidak's multiple comparison test, after ANOVA with factors of time and presence or absence of arabinose; **Figs. S13d** and **S13e**; see **Table S10** for full statistics). Additionally, researchers using theophylline have observed the need for screening their genes against putative aptamer sequences[11], to avoid naturally-occurring aptamers interacting with theophylline enough to interfere with translation and produce truncated proteins. Arabinose avoids this problem entirely; furthermore, the PBAD promoter is used in a great variety of commercially available bacterial expression vectors, many of which could be directly utilized in synells. Thus, arabinose shows great promise as a permeable activator for future liposomal genetically cascaded circuits.

Direct comparison of bacterial and mammalian systems

Synells containing mammalian and bacterial TX/TL, both systems expressing firefly luciferase, were compared side-by-side. The mammalian system was slower to reach maximum protein yield, and the total product yield was significantly lower, for the same volume and the same initial plasmid concentration (**Fig. S5**).

Typically, eukaryotic systems offer better folding and access to post-translational modifications, at the price of significantly lower yields[23]. Prokaryotic systems generally allow for higher yields at lower cost. If multi-domain proteins, complex signaling cascades, or large proteins are needed, eukaryotic systems generally should be used. Folding of large fusion proteins may be much more efficient in eukaryotic systems[24]. Also, eukaryotic systems typically offer a much wider range of post-translational modifications than prokaryotic extracts[25]. Bacterial extract, most commonly prepared form *E. coli*, is robust to changes in reaction temperature and tolerant to chemical additives while offering high yield of simple, unmodified proteins. Additionally, the bacterial TX/TL extract is relatively easy and cheap to prepare[26–30].

Mammalian cell-free TX/TL systems have been developed to synthesize long, complex proteins that require folding chaperones and post-translational modifications[23]. Commercially available rabbit reticulocyte systems offer cap-independent translation and contain mammalian folding chaperones. The glycosylation of proteins is possible in this system upon addition of canine pancreatic microsomal membranes; this typically decreases the overall yield of protein synthesis. Human HeLa cell extract is also commercially available; it is used to express antibodies, as well as large and complex proteins and viruses[31,32].

In summary, here is a brief general comparison of bacterial and mammalian systems (information based on several sources[23,28,33–35]; of course, these are generalities, and these rules of thumb may not always hold in all conditions):

	Bacterial	**Mammalian**
Protein yield	High yields	Low yields
Post-translational modifications	Very limited	Glycosylation possible, other modifications also possible
Cost of use	Low	High
Ease of use (tolerance to additives, temperature, etc.)	High: tolerance to extreme temperatures and small molecule additives	Low: narrower set of temperatures, sensitive to changes in conditions and composition of reaction mixture

Supplementary Figures

Fig. S1

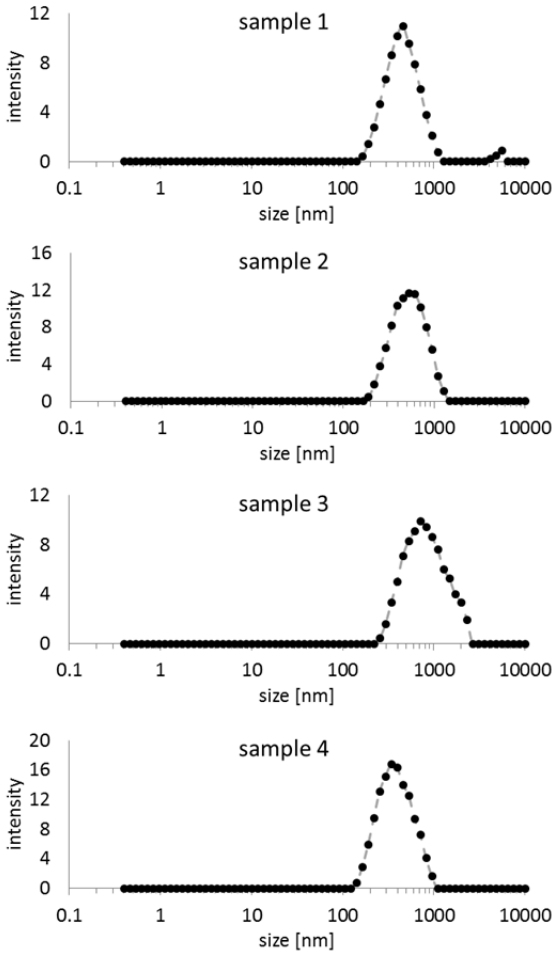

Fig. S1. Dynamic light scattering analysis of liposomes. We compared samples from separate encapsulation, extrusion and dialysis processes, prepared on different days. The measurements were performed using a Malvern Zetasizer Nano instrument, and data was analyzed using Zetasizer Ver. 7.04. All measurements were performed at 25°C, at measurement angle 173° backscatter.

Fig. S2

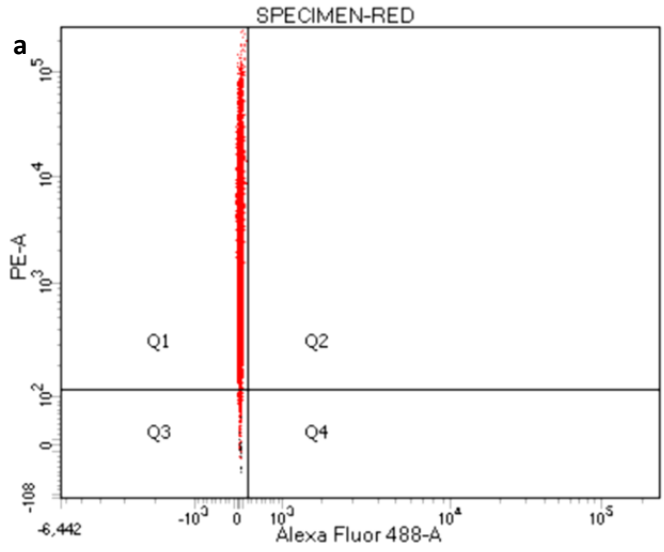
a
SPECIMEN-RED
PE-A
Q1
Q2
Q3
Q4
-6,442
Alexa Fluor 488-A

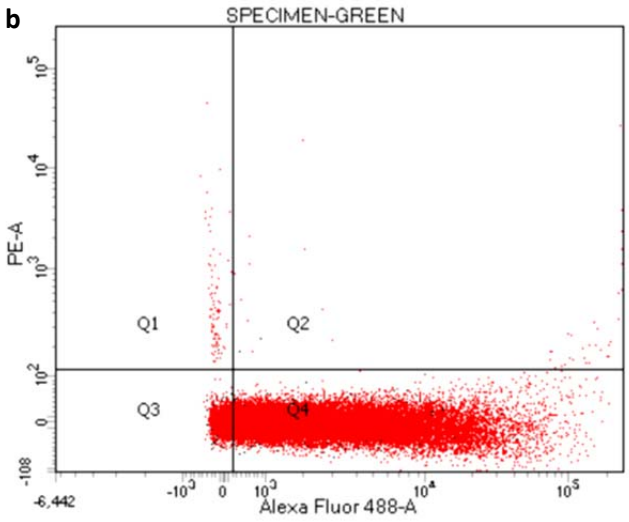
b
SPECIMEN-GREEN
PE-A
Q1
Q2
Q3
Q4
-6,442
Alexa Fluor 488-A

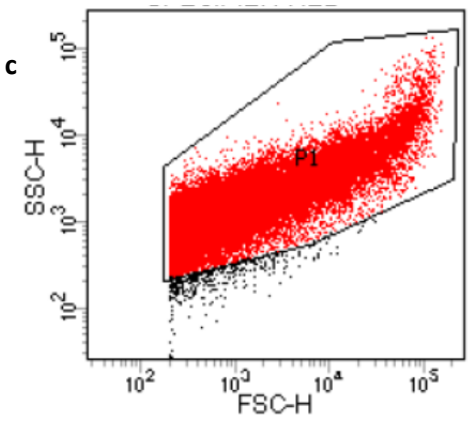

Fig. S2. Control samples for flow cytometry of synthetic minimal cells (as in **Figs. 2c** and **2d**). All samples contained liposomes with cell-free TX/TL mixture and a plasmid for expressing GFP, encapsulated in liposomes labeled with rhodamine-bearing membrane dye (red) prepared as described in **Materials and Methods**. **a.** Control red fluorescence sample: liposomes membrane-labeled with Lissamine Rhodamine B, without the GFP plasmid. The y-axis is fluorescence in the red (rhodamine) channel and the x-axis is fluorescence in the green (GFP) channel. **b.** Control green fluorescence sample: liposomes with T7-GFP plasmid; axes are as in **a**. Reaction conditions and plasmid concentrations are the same as in **Fig. 2**. The cytometry analysis was performed on FACSCanto II, and the data analysis was performed using FACSDiva 8.0. The red dots on the cytometry data on this figure and in **Fig. 2** represent counted events; the black dots represent events below the scattering threshold P1 (the threshold was set by the operator to eliminate events smaller than the typical size of dust in the sample); the same threshold applied to all datasets. **c.** Example of the scattering threshold size range; the y-axis is side scatter SSC-H and the x-axis is forward scatter FSC-H.

Fig. S3

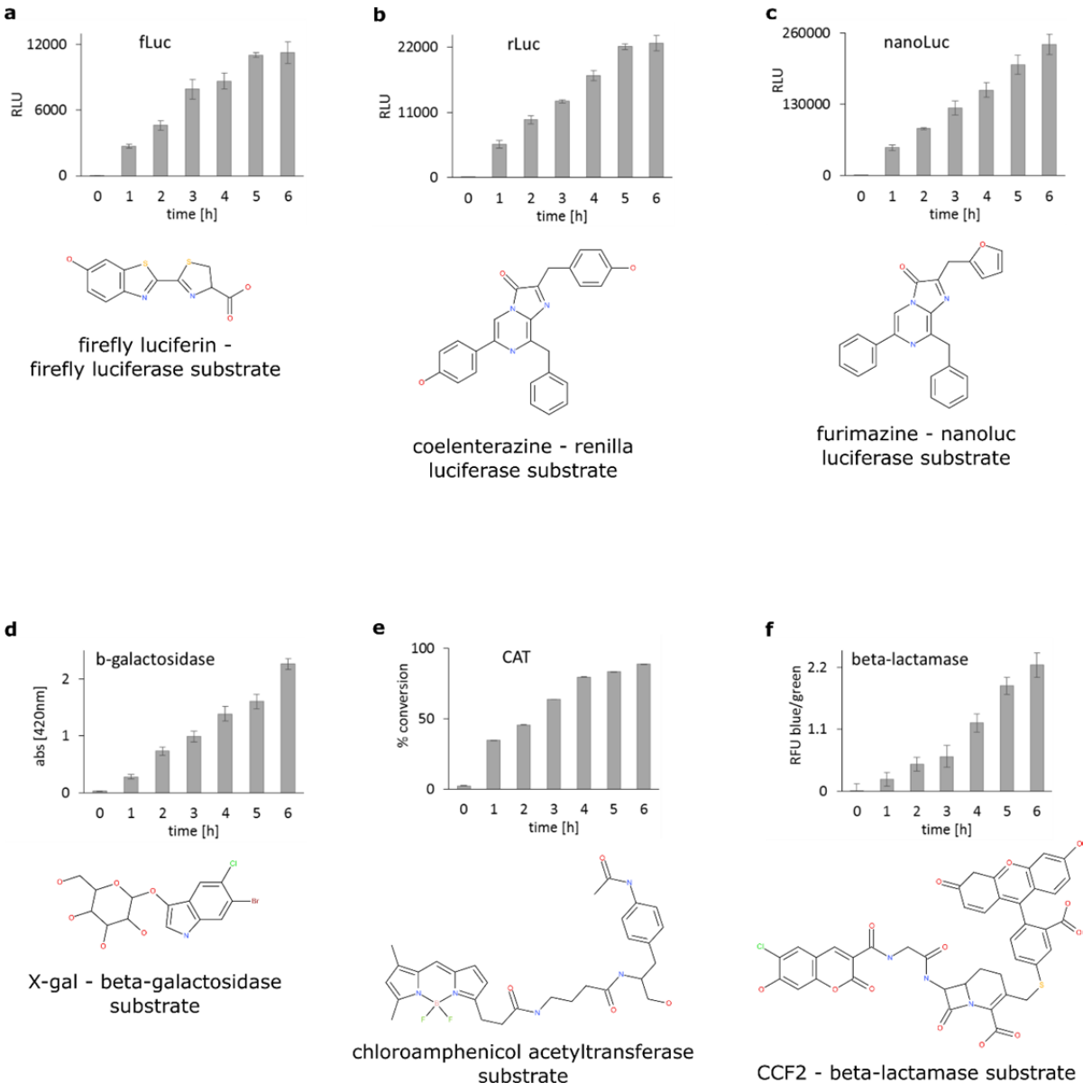

Fig. S3. T7-driven expression of enzymatic reporter proteins in synthetic cells. For each system, the substrate for the enzyme is also shown. **a.** Firefly luciferase. **b.** Renilla luciferase. **c.** NanoLuc luciferase. **d.** β-Galactosidase. **e.** Chloramphenicol acetyltransferase. **f.** β-lactamase. All constructs were under the P70 promoter, expressed in bacterial cell-free TX/TL extract according to the procedure described in **Materials and Methods**. All 6 enzymes were analyzed according to the protocols from the assay kits

used for each enzyme—see **Materials and Methods** for details. Each reaction was stopped at the indicated time point and processed according to the protocol for each enzyme assay kit. Error bars in panels **a, b, c,** and **d** indicate S. E. M., error bars in panels **e** and **f** indicate error propagated from the standard deviation of two wavelength signals. All data points are an arithmetic average of 3 replicates.

Fig. S4

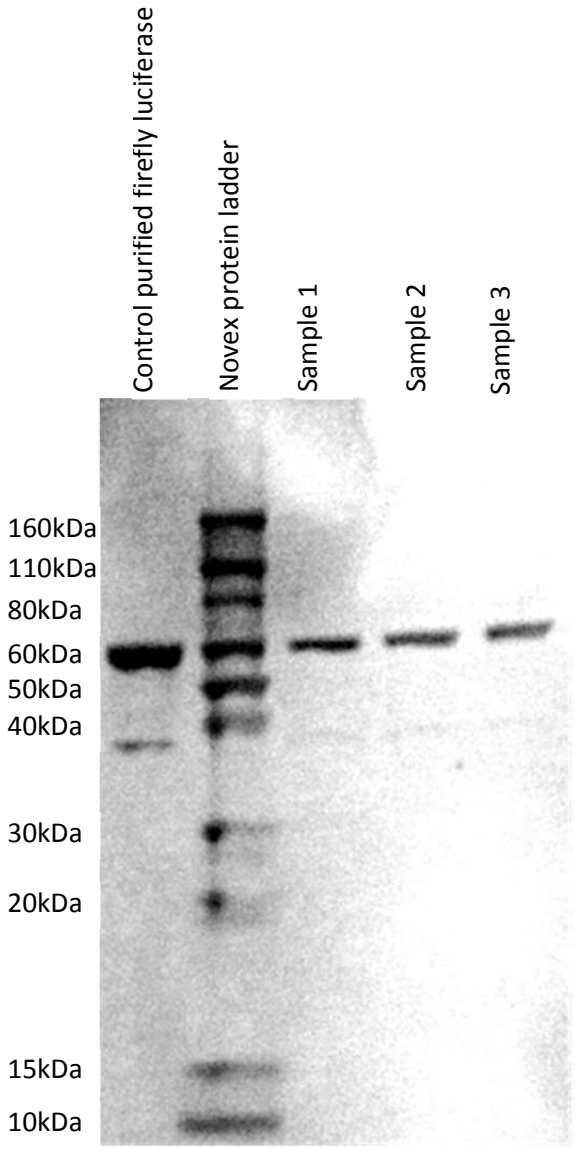

Fig. S4. Western blot analysis of firefly luciferase expression. Protein chromatography was performed using Novex™ 14% Tris-Glycine Mini Protein Gels; primary antibody staining was performed with mouse monoclonal Anti-6X His tag antibodies (Abcam); and secondary staining was performed using WesternBreeze Chromogenic Kit, anti-mouse (Thermo Scientific). **Sample 1**: Firefly luciferase expression under T7 promoter in a bacterial TX/TL system. **Sample 2**: Firefly luciferase expression under

the Tet promoter in a bacterial TX/TL system. **Sample 3**: Luciferase expression in a HeLa TX/TL system after transcription using HeLa nuclear extract. The sample used in this experiment is the same as in the 1:1 A:B ratio in **Fig. 6f**. Prior to loading of the gel, luciferase activity in aliquots of each sample was measured, and the obtained luminescence signal was used to approximately normalize the concentration (loading volume) of all samples. As a positive control, purified full-length recombinant firefly luciferase protein (Abcam) was used.

Fig. S5

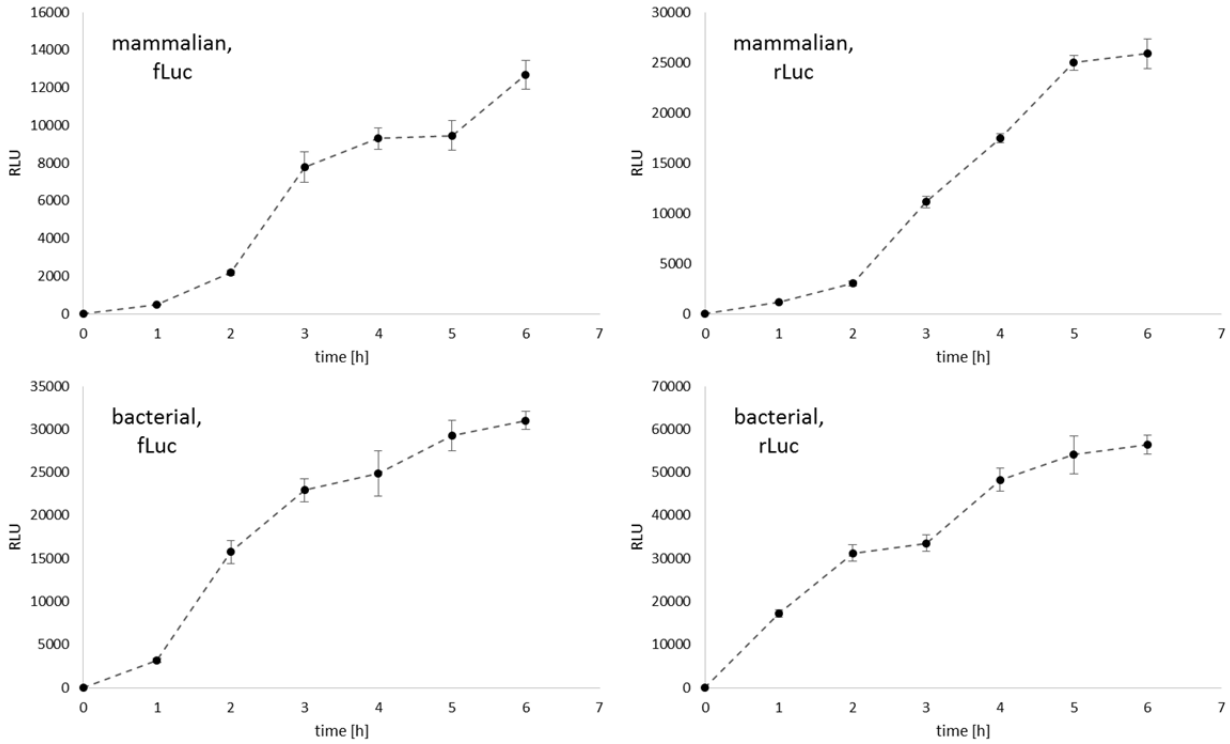

Fig. S5. Comparison of bacterial and mammalian TX/TL, for firefly and Renilla luciferases (fLuc and rLuc). Dotted lines are visual guides, not data fits. Error bars indicate S. E. M., n=4.

Fig. S6

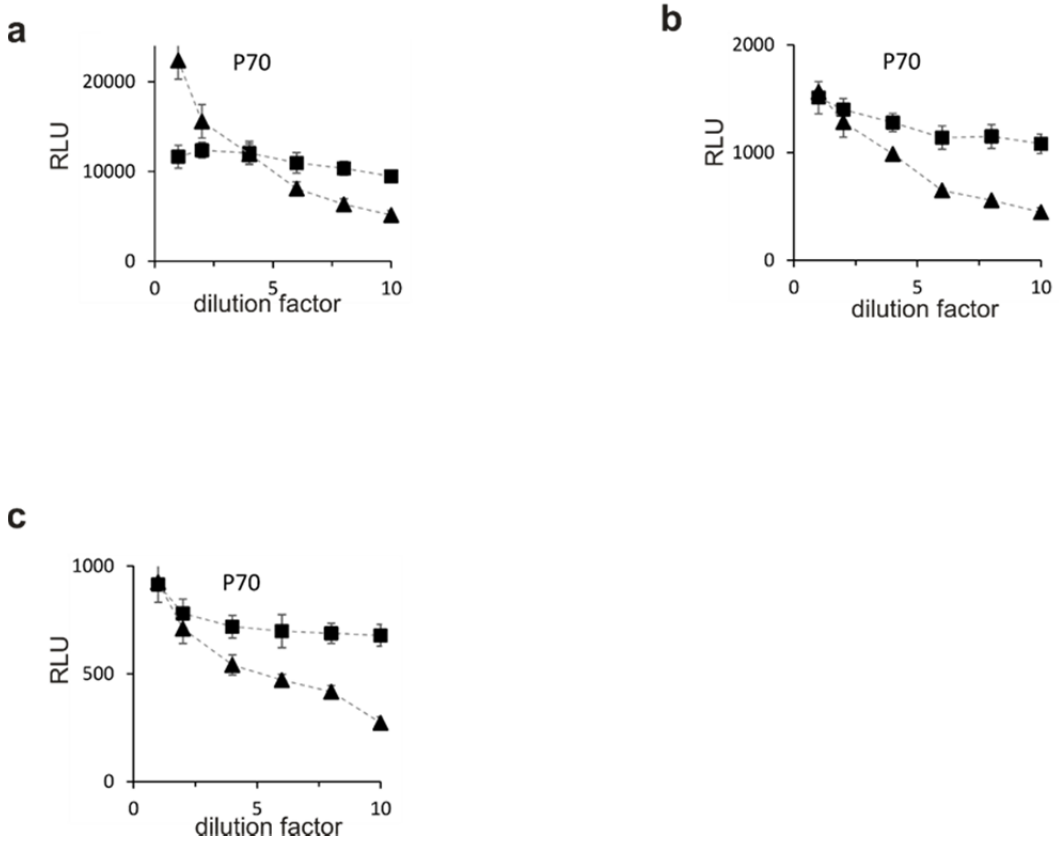

Fig. S6. Effects of dilution on fLuc expression in liposomes and unencapsulated reactions. Expression of one-, two-, and three-peptide systems under control of the P70 promoter, without small molecule activation. **a.** One-part luciferase system (as in **Fig. 3d**). **b.** Two-part split luciferase system (as in **Fig. 3e**). **c.** Three-part scaffolded split luciferase system (as in **Fig. 3f**).

Fig. S7

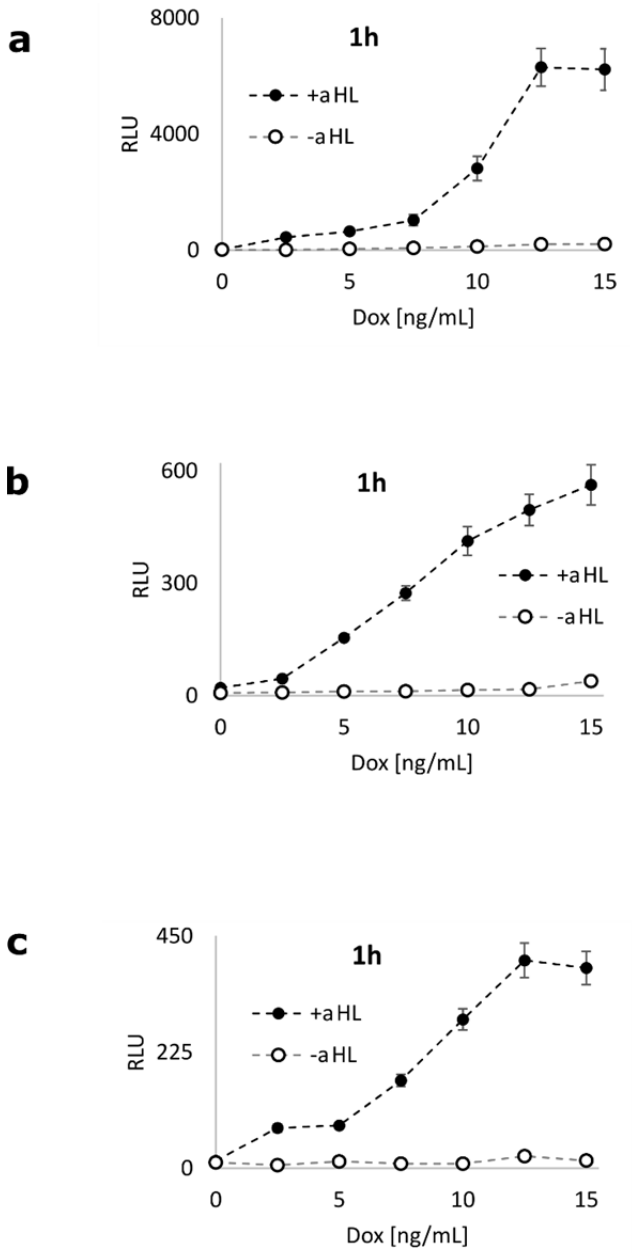

Fig. S7. End-point expression of luciferase from each of the expression systems presented in **Fig. 3**, measured at end point 1 h, at 7 different concentrations of Dox. The dotted lines are visual guides, not fits. **a.** One-part luciferase system (as in **Fig. 3g**). **b.** Two-part split luciferase system (as in **Fig. 3h**). **c.** Three-part scaffolded split luciferase system (as in **Fig. 3i**).

Fig. S8

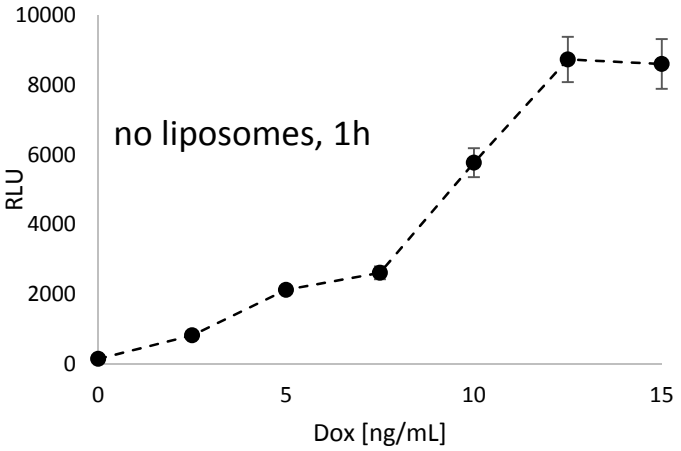

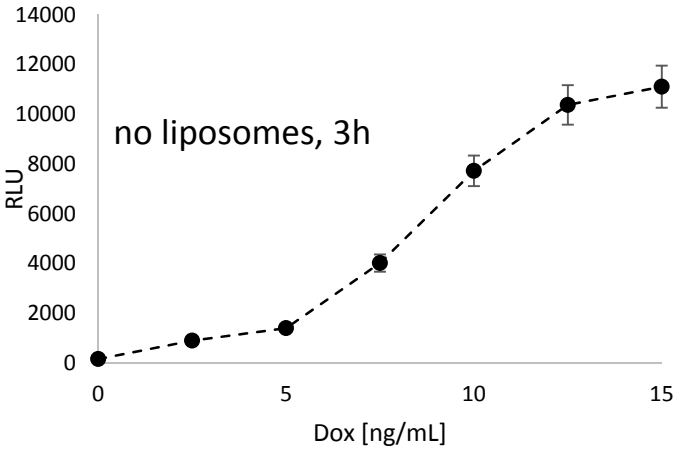

Fig. S8: Single-protein fLuc expression in solution (as in **Fig. 3g**), 5 nM plasmid.

Fig. S9

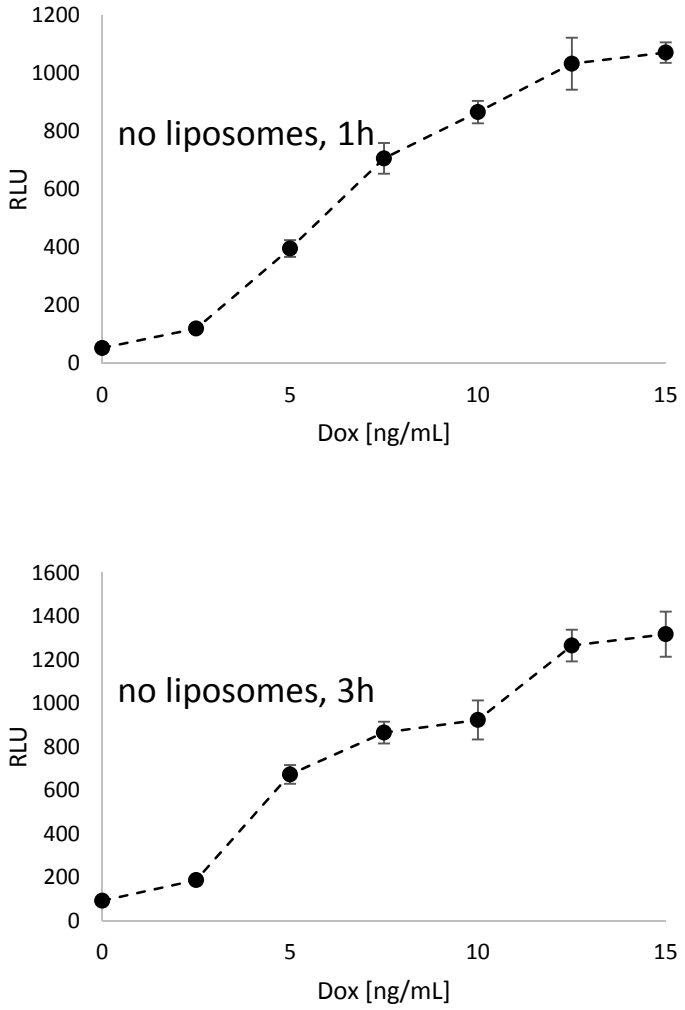

Fig. S9: Two-protein fLuc expression in solution, plasmids for fLucA and fLucB combined at 2.5 nM each (as in **Fig. 3h**).

Fig. S10

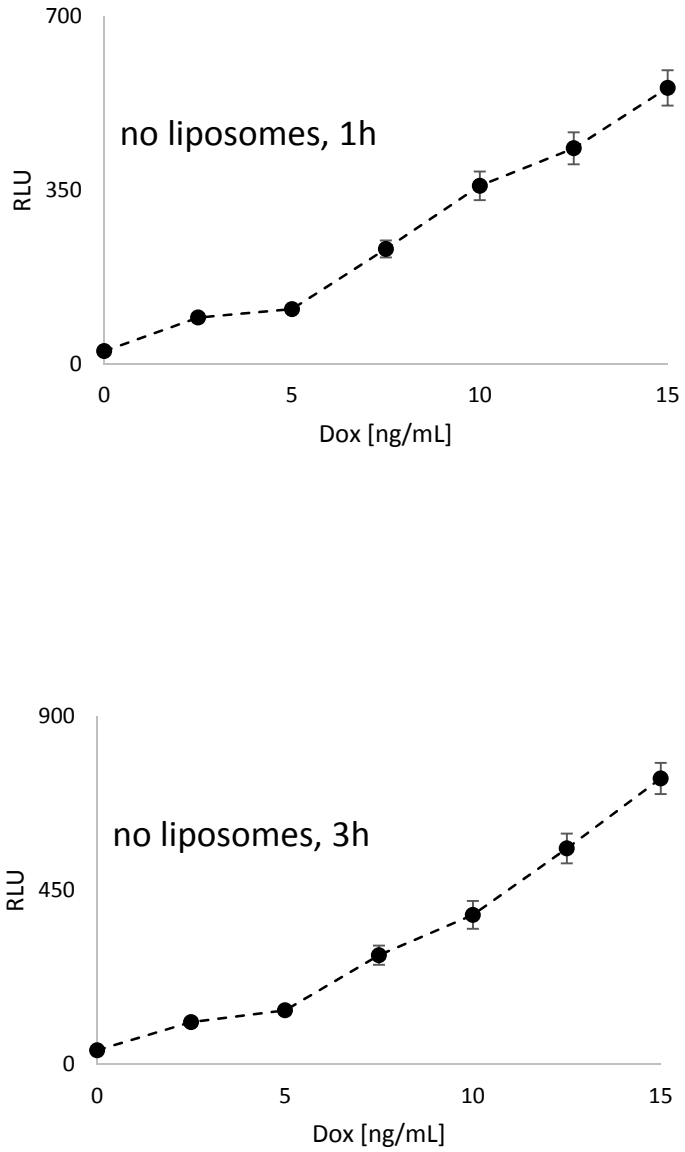

Fig. S10: Three-protein fLuc expression in solution; plasmids fLucC, fLucD, and Scaffold combined at 1.67 nM each (as in **Fig. 3i**).

Fig. S11

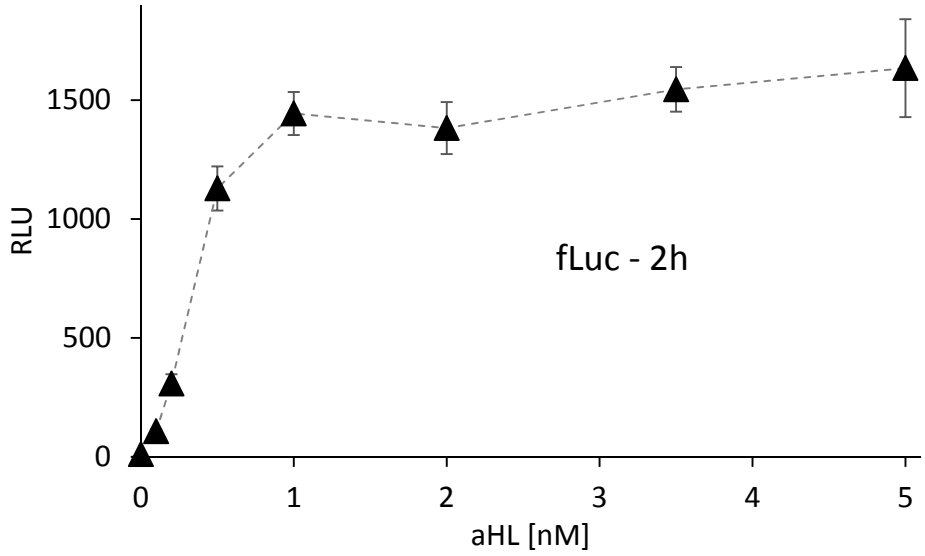

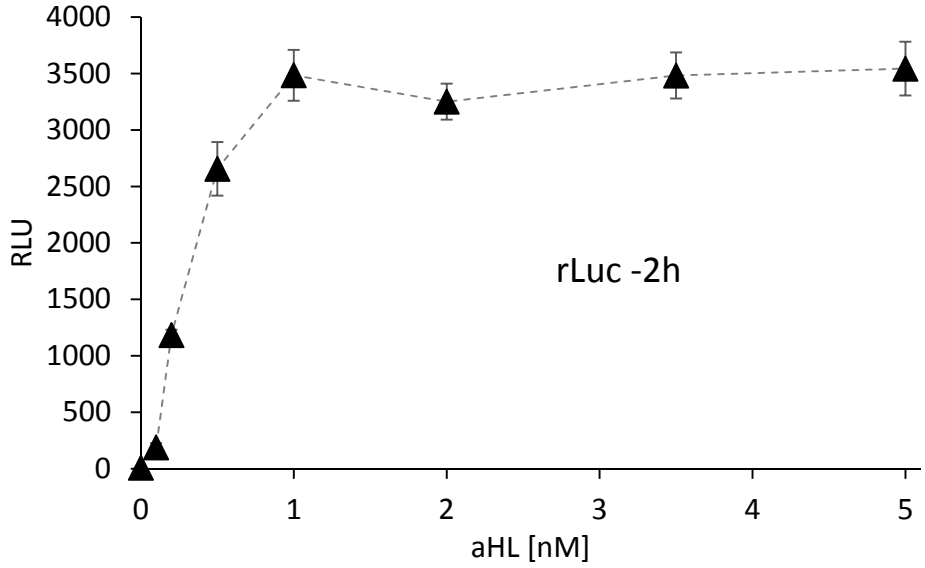

Fig. S11: Expression of fLuc and rLuc at 2 h end-point, from liposomes with different concentration of aHL plasmid (as in **Fig. 4**).

Fig. S12

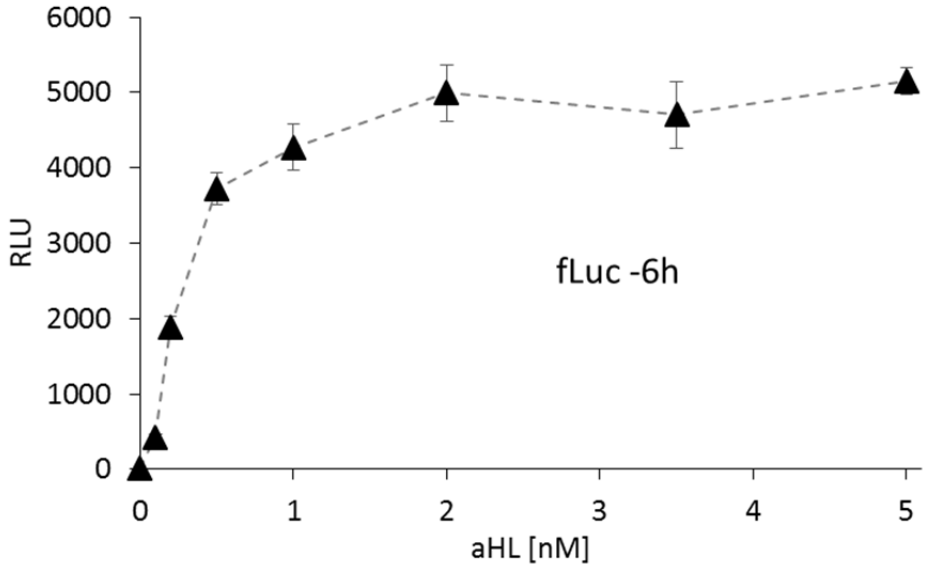

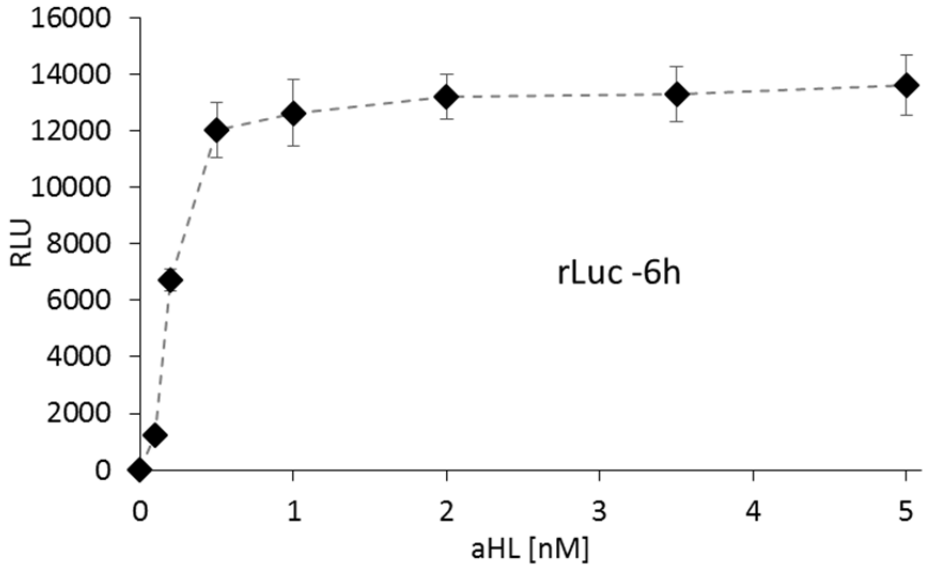

Fig. S12: Expression of fLuc and rLuc at 6 h end-point, from liposomes with different concentration of aHL plasmid (as in **Fig. 4**).

Fig. S13

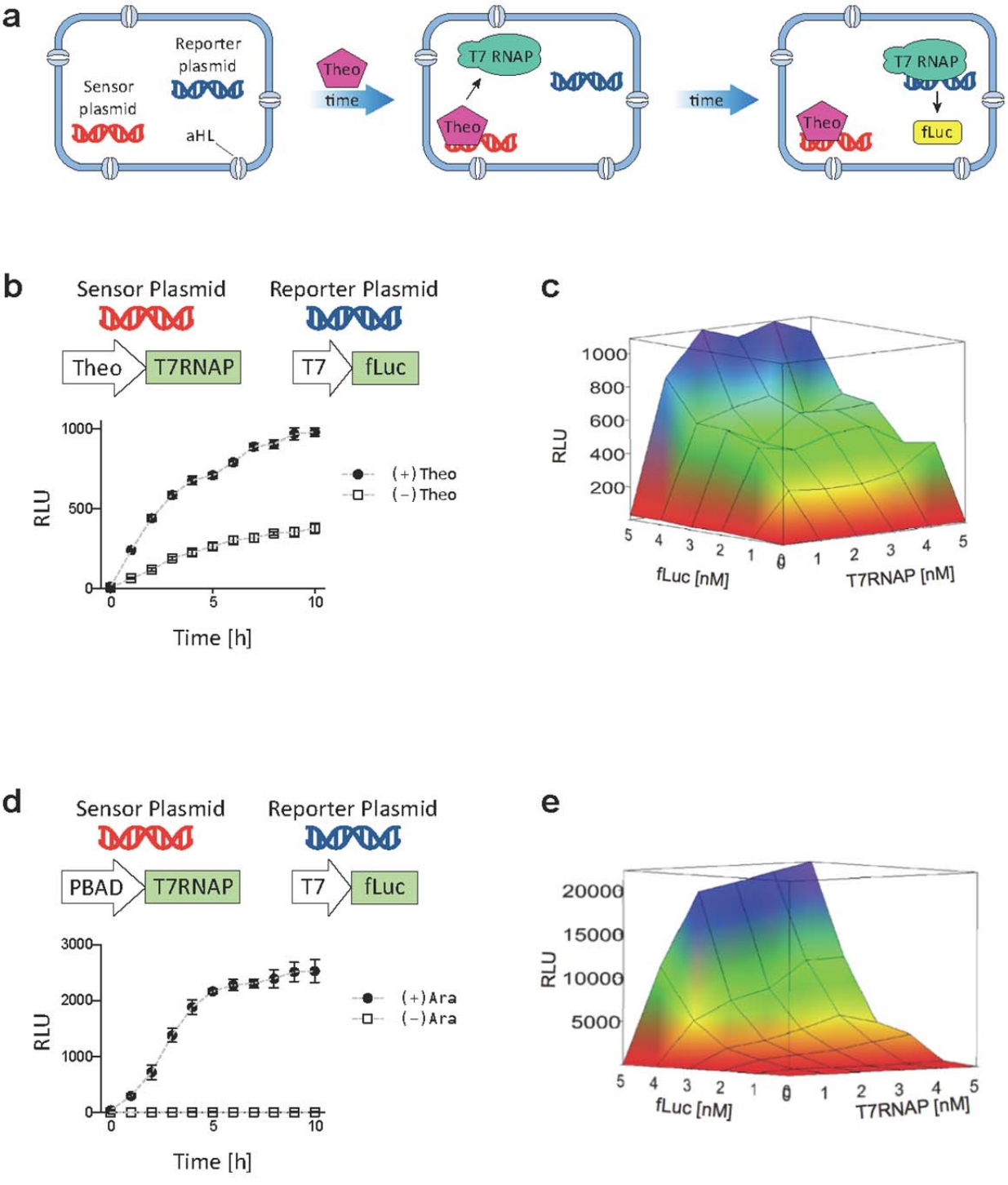
a
Sensor plasmid
Reporter plasmid
aHL
Theo
time
T7 RNAP
Theo
time
T7 RNAP
Theo
fLuc
b
Sensor Plasmid
Reporter Plasmid
Theo
T7RNAP
T7
fLuc
RLU
1000
500
0
0
5
10
Time [h]
(+) Theo
(−) Theo
c
RLU
1000
800
600
400
200
5 4 3 2 1 0 1 2 3 4 5
fLuc [nM]
T7RNAP [nM]
d
Sensor Plasmid
Reporter Plasmid
PBAD
T7RNAP
T7
fLuc
RLU
3000
2000
1000
0
0
5
10
Time [h]
(+) Ara
(−) Ara
e
RLU
20000
15000
10000
5000
5 4 3 2 1 0 1 2 3 4 5
fLuc [nM]
T7RNAP [nM]

Fig. S13. Activation of liposomally encapsulated cascaded genetic networks via membrane-permeable small molecules. a. Schematic of synthetic minimal cells created. The liposomes used in this figure were built with bacterial transcription/translation (TX/TL) components; they contain the gene for T7 RNA Polymerase (T7RNAP) under an inducible element—either the Theo aptamer, which responds to theophylline (Theo), or the PBAD promoter, which responds to arabinose (Ara)—and the gene for firefly luciferase (fLuc) under a T7 promoter. A small molecule activator (Theo or Ara) drives T7RNAP expression, which in turn drives fLuc expression. **b-c.** The theophylline-triggered genetic cascade. **b.** fLuc expression over time, with and without 2 mM Theo; each of the two plasmids is present at 5 nM. **c.** Final fLuc expression at different concentrations of each plasmid, all measured after 10 h of expression. **d-e.** The arabinose-triggered genetic cascade. **d.** fLuc expression over time, with and without 10 mM Ara; each of the two plasmids is present at 5 nM. **e.** Final fLuc expression at different concentration of each plasmid, all measured after 10 h of expression. All data points are an average of 4 replicates; error bars indicate S. E. M.

Fig. S14

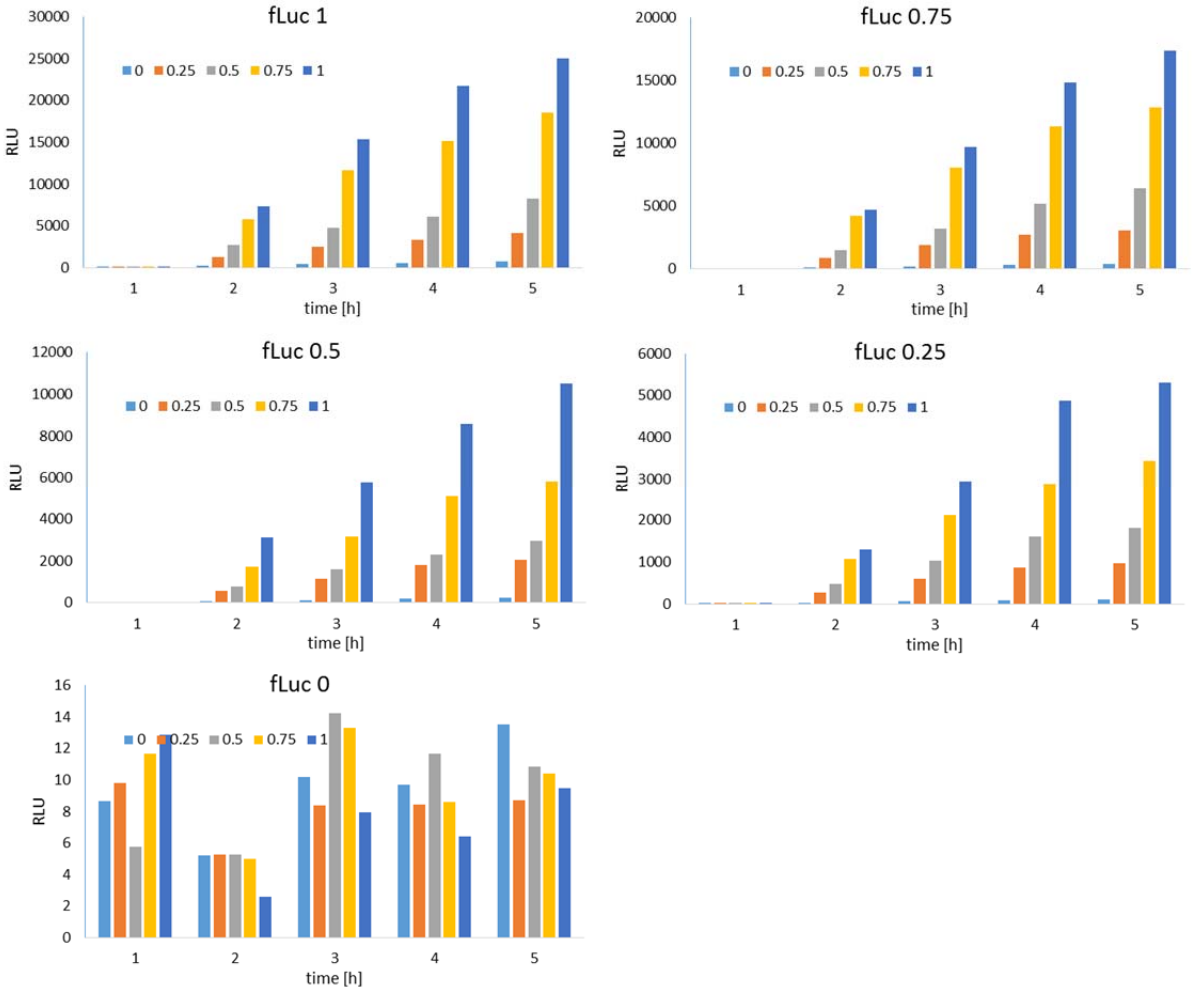

Fig. S14: Time-course of expression of fLuc under the lac promoter, with different ratios of liposomes (as in **Fig. 5c**). Occupancies are numerically defined as in the legend for **Fig. 5**.

Fig. S15

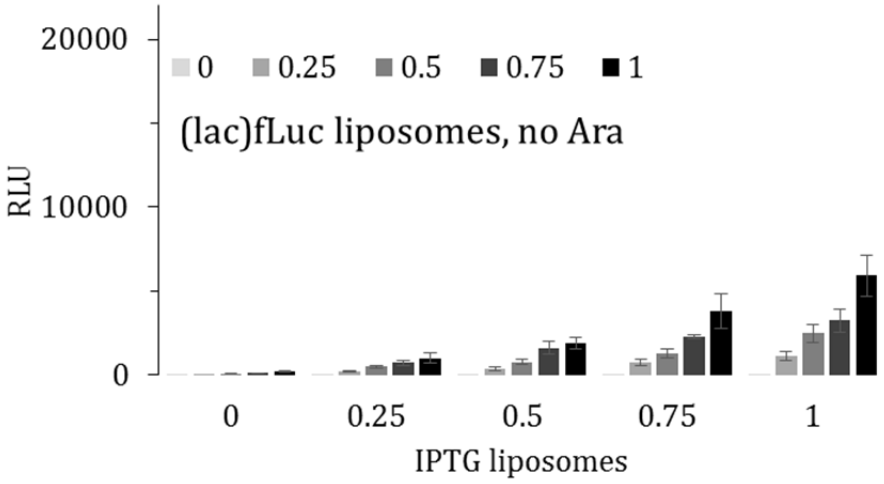

Fig. S15. Expression of fLuc under lac promoter in absence of arabinose (as in **Fig. 5c**). Occupancies are numerically defined as in the legend for **Fig. 5**.

Fig. S16

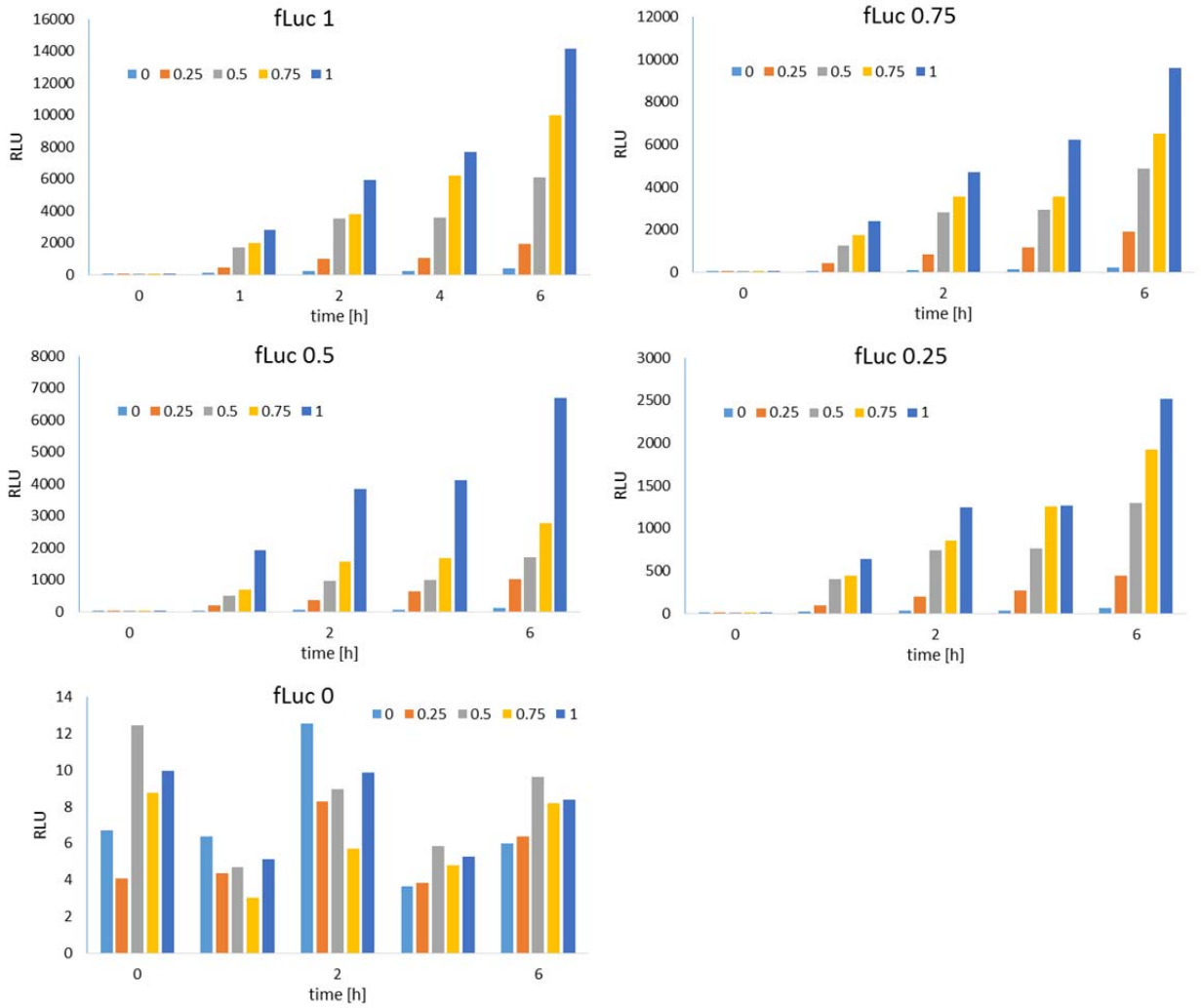

Fig. S16: Time course of fLuc under T7 promoter, driven by T7RNAP under the lac promoter, with different ratios of liposomes (as in **Fig. 5d**). Occupancies are numerically defined as in the legend for **Fig. 5**.

Fig. S17

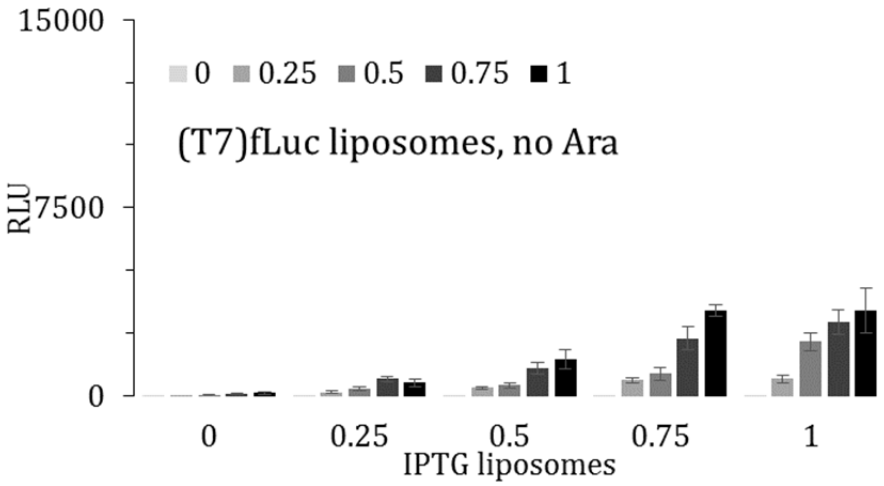

Fig. S17. Expression of fLuc under the T7 promoter, driven by T7RNAP under the lac promoter, in the absence of Arabinose (as in **Fig. 5d**). Occupancies are numerically defined as in the legend for **Fig. 5**.

Fig. S18

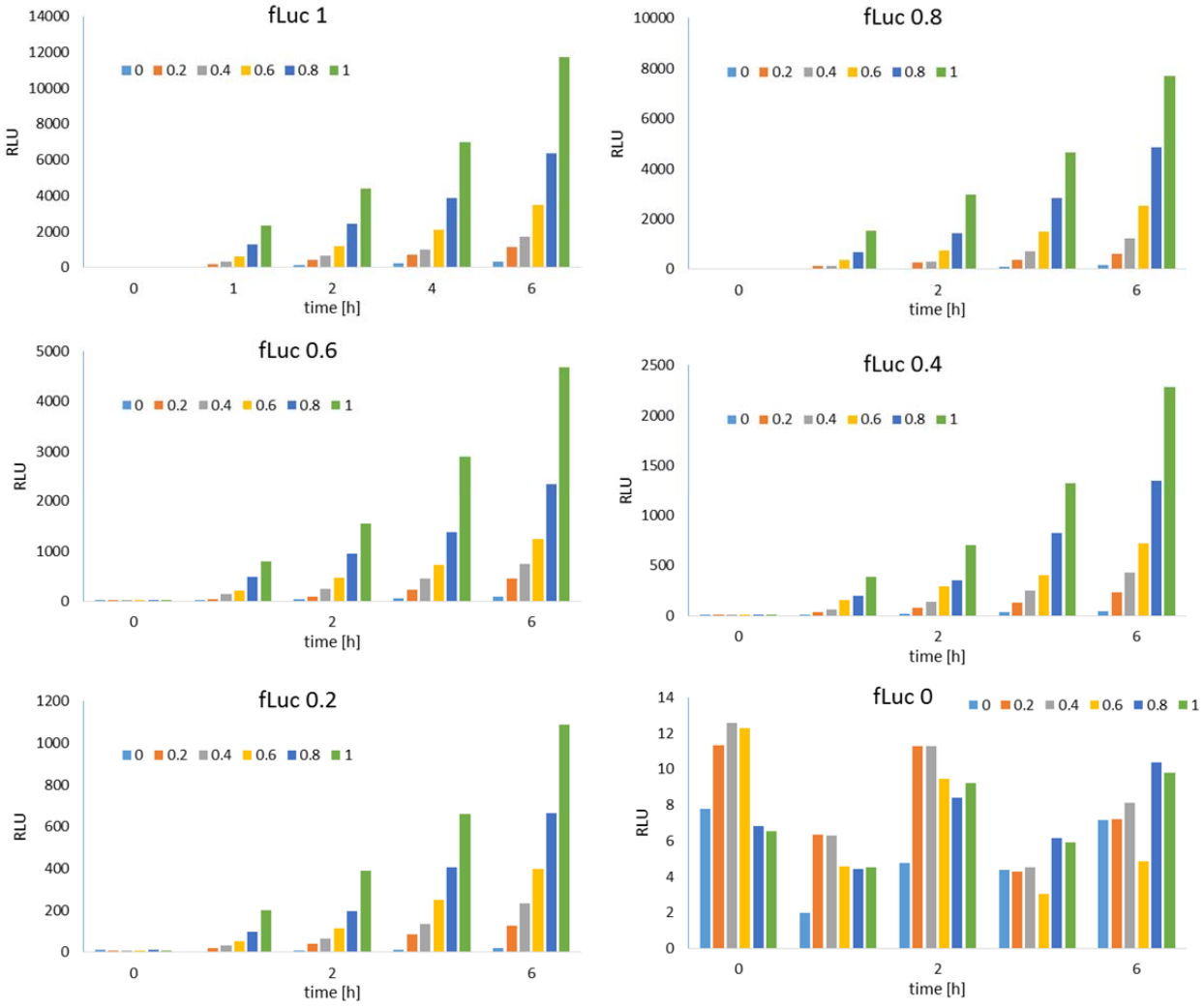

Fig. S18. Time course of fLuc expression at different ratios of fLuc and Tet liposomes (as in **Fig. 5f**). Occupancies are numerically defined as in the legend for **Fig. 5**.

Fig. S19

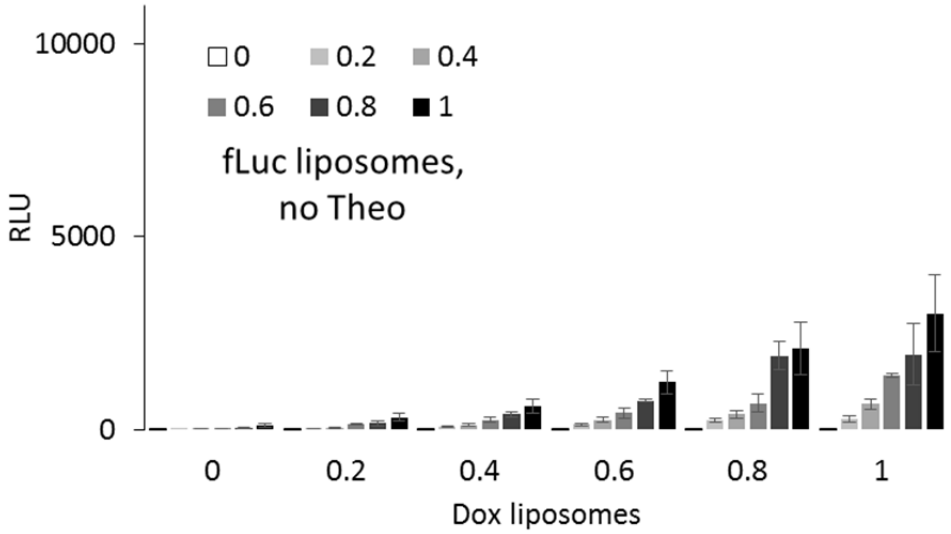

Fig. S19: End-point data for fLuc expression without theophylline (as in **Fig. 5f**). Occupancies are numerically defined as in the legend for **Fig. 5**.

Fig. S20

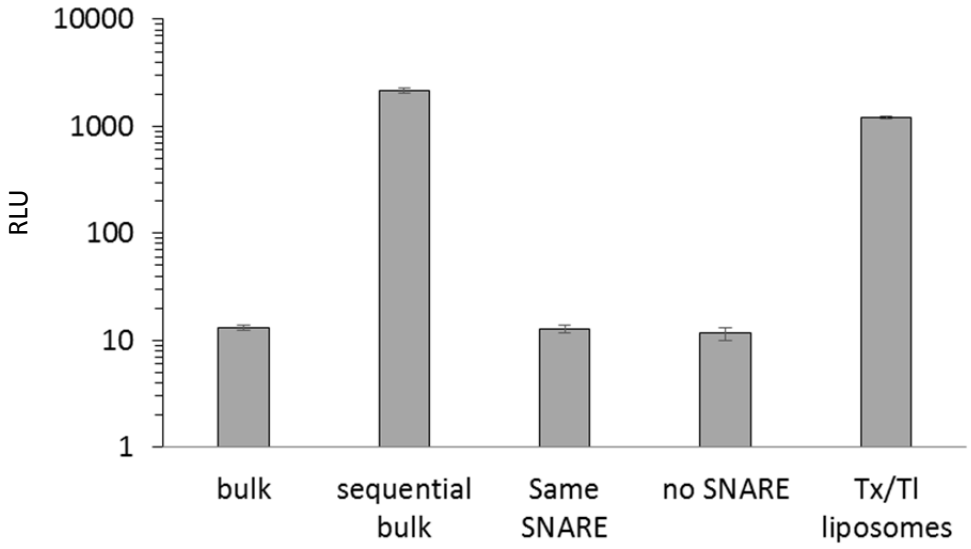

Fig. S20. Cell-free transcription and translation in mammalian cell-free systems. From left to right, the bars correspond to:

Bulk: cell-free TX and TL systems, same as used in experiments presented in **Fig. 6f**, but mixed in one tube instead of encapsulating in separate liposomes, and incubated for 24 hours at 37°C.

Sequential bulk: the TX reaction incubated for 12 hours, then mixed with equal volume of the TL mixture, incubated for another 12 hours (like experiment of **Fig. 6f**, but without liposome encapsulation).

Same SNARE, no SNARE and TX/TL liposomes are the same data as presented on **Fig. 6f**, shown here again for reference.

Fig. S21

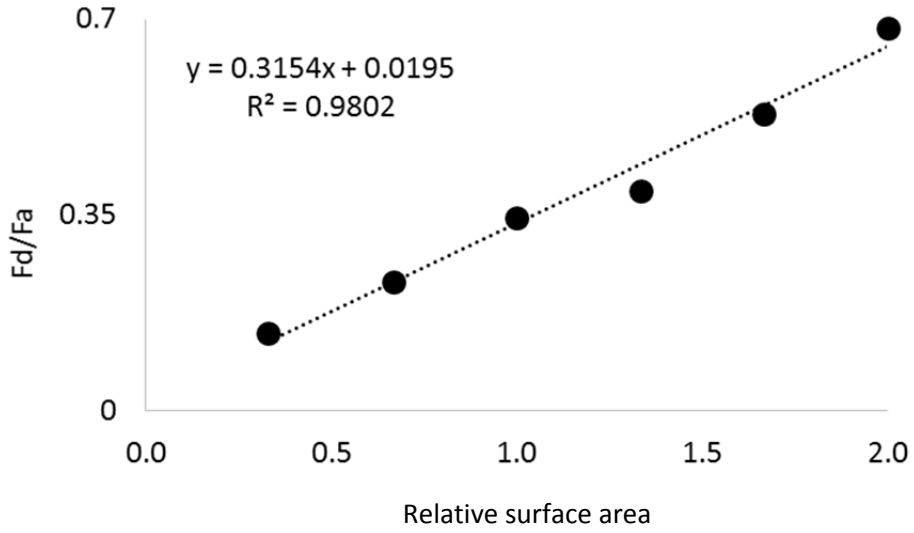

Fig. S21. Calibration curve for FRET response. The samples were prepared with varying ratios of the FRET dye pair lipids (Lissamine™ Rhodamine B 1,2-Dihexadecanoyl-sn-Glycero-3-Phosphoethanolamine, Triethylammonium Salt and NBD-PE (N-(7 Nitrobenz-2-Oxa-1,3-Diazol-4-yl)-1,2-Dihexadecanoyl-sn-Glycero-3-Phosphoethanolamine, Triethylammonium Salt)) to the POPC:cholesterol lipid mix, in order to mimic surface area change in fusion experiments. Fd, fluorescence of donor; Fa, fluorescence of acceptor; the relative surface area of 1 is defined as the starting ratio of FRET dyes to lipids in the SNARE fusion experiment samples, and subsequent values of surface are obtained by scaling proportionally (increasing or decreasing) the concentration of FRET dyes in the membrane, as described previously.[36,37]

Fig. S22

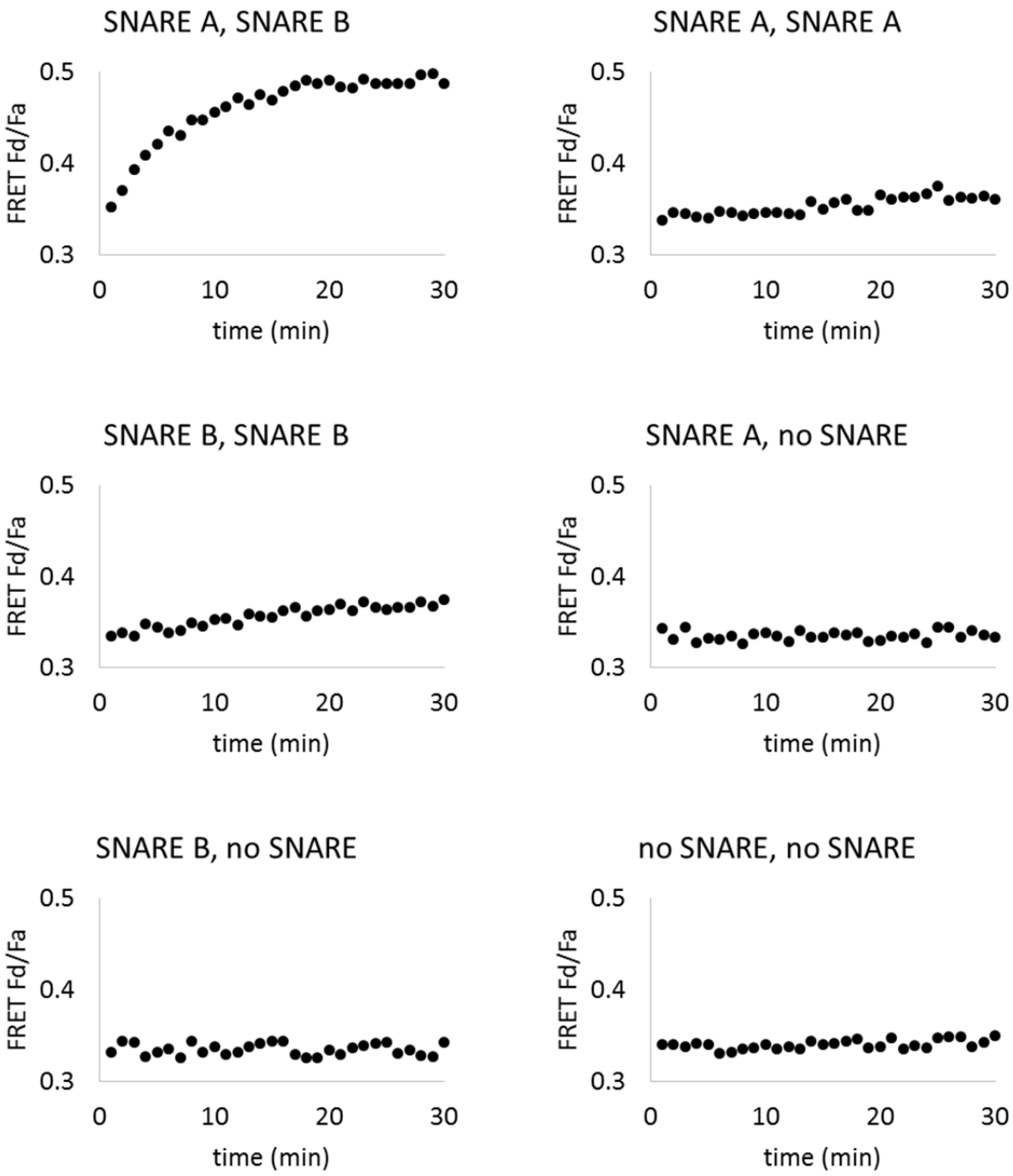

Fig. S22. Liposome fusion induced by SNARE protein mimics. The mixing of liposomes was measured with changes of FRET signal from the FRET donor and acceptor dyes in the liposomes, both to confirm mixing and as a way to estimate the time course of vesicle size increases due to fusion. For experimental details, see **Materials and Methods**. The letters A and B represent a pair of SNAREs that bind to one another; when A is paired with A, or B with B, no binding or fusion happens.

Fig. S23

sample	**1**	**2**	**3**	**4**	**5**	**6**
probe	SNARE A	SNARE B	SNARE A	SNARE A	SNARE B	SNARE B
positive target	SNARE B	SNARE A	SNARE A	no SNARE	SNARE B	no SNARE
sample	**7**	**8**	**9**	**10**	**11**	**12**
probe	SNARE A	SNARE B	SNARE A	SNARE A	SNARE B	SNARE B
negative target	SNARE B	SNARE A	SNARE A	no SNARE	SNARE B	no SNARE

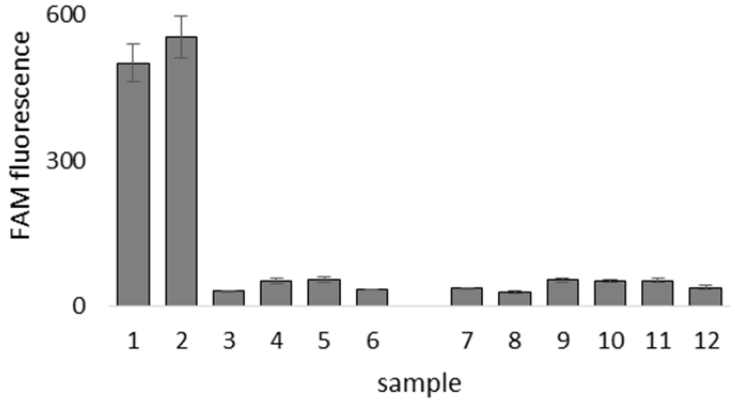

Fig. S23. De-quenching of a liposome-encapsulated molecular beacon upon SNARE mediated fusion with liposomes encapsulating a complementary target. Molecular beacon FAM-5'-GCGAGCTAGGAAACACCAAAGATGATATTTGCTCGC -3'-DABCYL was encapsulated in one population of liposomes ("probe" liposomes), and a complementary target ("positive target") or a non-complementary target ("negative target") were encapsulated in the other population of liposomes. Liposomes were prepared and purified according to the general procedures described in **Material and Methods**. Samples were then mixed, incubated for 30 min at room temperature, and fluorescence of the fluorescein (FAM) dye was measured. The increased fluorescence indicates de-quenched FAM probe as a result of hybridization of a molecular beacon to the target sequence, and thus mixing of the content of the liposomes upon SNARE-mediated fusion. Error bars indicate S.E.M. n=3.

Fig. S24

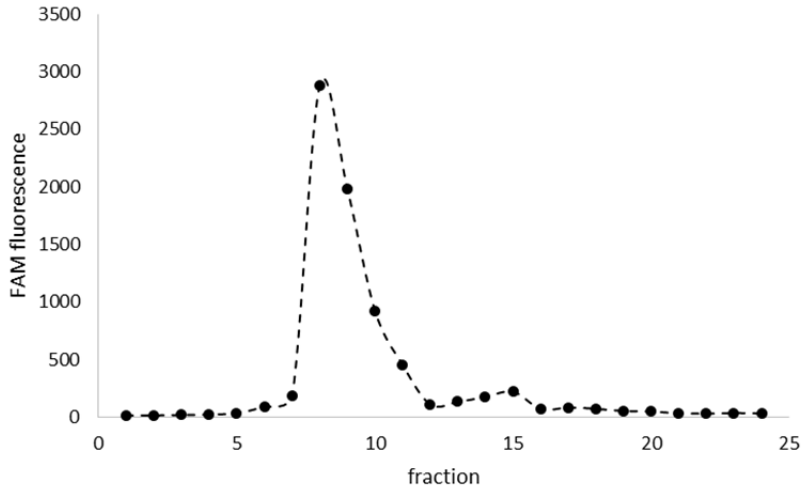

Fig. S24. Leakage of DNA oligonucleotide from liposomes after SNARE-induced fusion. The fluorescent oligonucleotide 5'-FAM-d(GCG CAT TGG)-3' was encapsulated at 1 μM in both populations of liposomes containing SNARE A and SNARE B (a matched pair, as defined in **Fig. 6a**). The liposomes were extruded and purified as described in **Materials and Methods**, and fusion reactions were performed. After fusion and 1 h equilibration, the sample was purified on a Sepharose 4B size-exclusion column. The combined total free-molecule fraction fluorescence is about 8.2% of the total fluorescence measured from all liposome and free-molecule fractions (we defined the liposome fraction as the sum of fractions 6 to 12, and the free-molecule fraction as the sum of fractions 13 to 17).

Fig. S25

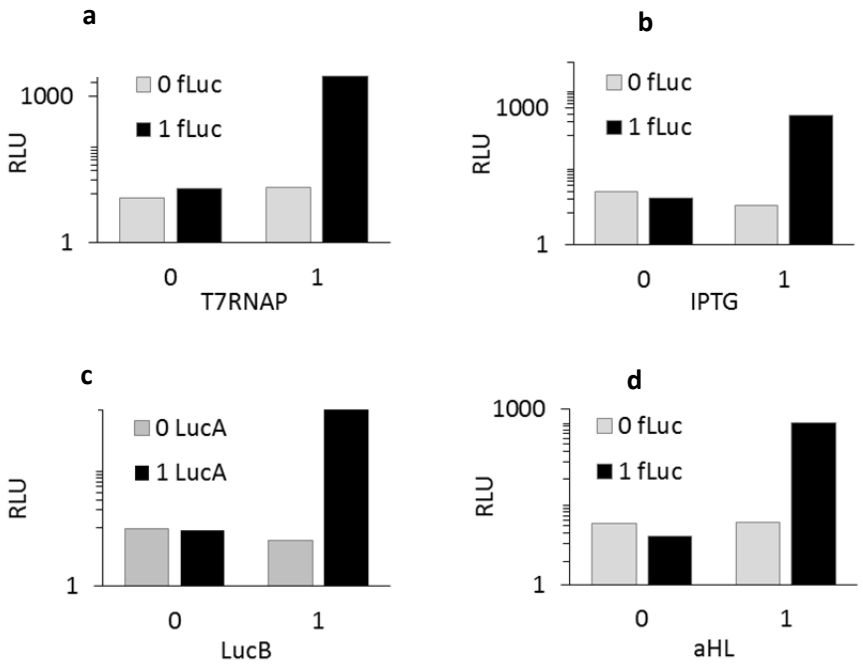

Fig. S25: Fusion of liposomes and subsequent merging of independent genetic circuits using SNARE protein mimics—with liposome pairs reversed compared to the experiments shown in **Fig. 6**. These experiments were designed analogously to the results presented in **Fig. 6**: two populations of liposomes were prepared, each with one of the SNARE protein mimics (see **Fig. 6a** for the experimental setup). Equal volumes of each population were mixed, containing two different concentrations of the liposomes: 10 mM (1) or zero (0), resulting in 4 different ratios of liposomes tested. All samples were incubated for 6 h after mixing, after which end-point fLuc luminescence was analyzed as described in **Materials and Methods**. **a.** Cascading genetic circuit of **Fig. 6b** with flipped SNAREs: T7RNAP under the P70 promoter (SNARE_B) mixed with fLuc under T7 promoter (SNARE_A). **b.** Delivering small molecule activator: fLuc under lac promoter (SNARE_B) mixed with IPTG-filled liposomes (SNARE_A), as in **Fig. 6c** but with flipped SNAREs. **c.** Creating protein reconstitution system: fLucA (SNARE_B) mixed with fLucB (SNARE_A), as in **Fig. 6e** but with flipped SNAREs. **d.** Enabling small molecule activation: liposomes expressing aHL (SNARE_B) mixed with fLuc under lac promoter (SNARE_A), IPTG added to the external solution, as in **Fig. 6d** but with SNAREs flipped.

Fig. S26

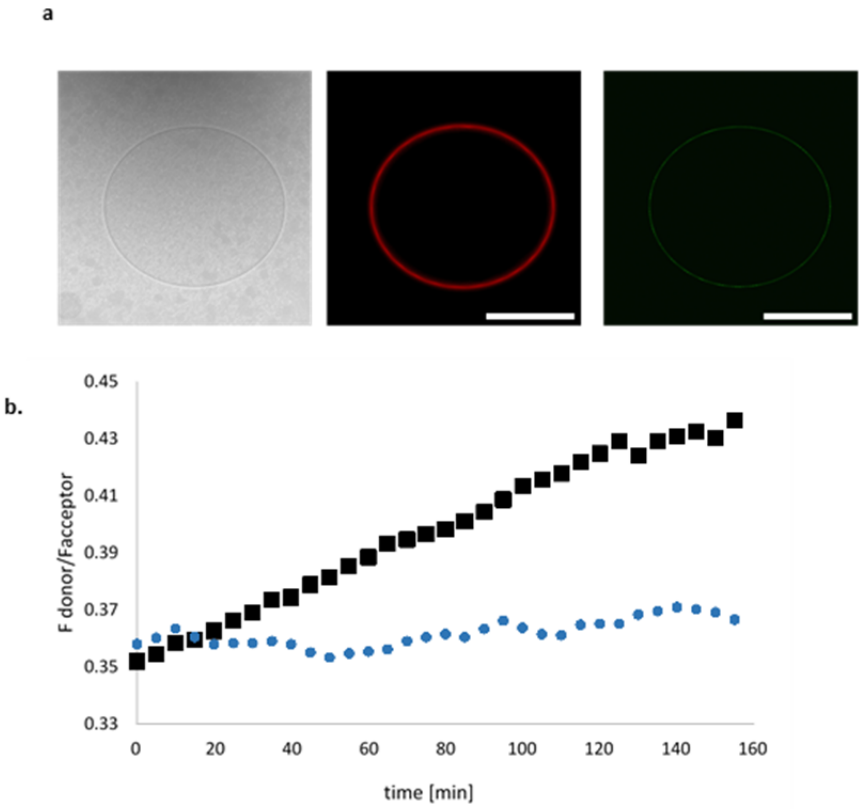

Fig. S26: Incorporation of alpha hemolysin protein into phospholipid bilayer membrane. **a** Confocal microscopy images of liposome expressing alpha hemolysin—mClover protein fusion, with liposome membrane labeled with red dye (rhodamine functionalized with a lipid tail, Lissamine rhodamine B). Giant unilamellar vesicles were prepared according to previously described methods[19], and non-encapsulated TL/TL mixture was removed by dialysis as described in **Materials and Methods.** The scale bar is 5µm. **b**. Incorporation of alpha hemolysin protein in the bilayer membrane of the phospholipid liposome is measured by FRET (Fluorescence Resonance Energy Transfer). The membrane is labeled with two FRET pair dyes: Lissamine Rhodamine B 1,2-Dihexadecanoyl-sn-Glycero-3-Phosphoethanolamine, Triethylammonium Salt and NBD-PE N-(7 Nitrobenz-2-Oxa-1,3-Diazol-4-yl)-1,2-Dihexadecanoyl-sn-Glycero-3-Phosphoethanolamine, Triethylammonium Salt. The alpha hemolysin was constituently expressed inside liposomes using a bacterial TX/TL system and the bacterial P70 promoter (black squares); as a control a soluble, non-membrane associated protein (firefly luciferase) was expressed under the same conditions (blue circles).

Supplementary Tables

Abbreviations

Common abbreviations used throughout the **Supplementary Tables**:

Abbreviation	Meaning
Diff.	Difference
ns	Not significant
CI	Confidence interval
Nparm	Number of parameters
DF	Degrees of freedom
*	Significant
****	More significant

Table S1

Statistics for **Fig. 3d**: 2-way ANOVA with factors of "Dilution Factor" and "Encapsulation".

Source of Variation	% of total variation	P value	P value summary	Significant?
Interaction	29.8	< 0.0001	****	Yes
Dilution Factor	57.94	< 0.0001	****	Yes
Encapsulation	3.859	0.0002	***	Yes

Dunnett's multiple comparisons test after the ANOVA.

	Mean Diff.	95% CI of diff.	Significant?	Summary	Adjusted P Value
Liposome					
2 vs. 1	-500.6	-1552 to 551.2	No	ns	0.6003
4 vs. 1	-496	-1548 to 555.9	No	ns	0.6084
6 vs. 1	-1005	-2057 to 46.55	No	ns	0.0652
8 vs. 1	-1106	-2158 to -54.09	Yes	*	0.0364
10 vs. 1	-913.1	-1965 to 138.7	No	ns	0.1071
Solution					
2 vs. 1	-2631	-3683 to -1579	Yes	****	< 0.0001
4 vs. 1	-3916	-4968 to -2865	Yes	****	< 0.0001
6 vs. 1	-5429	-6481 to -4378	Yes	****	< 0.0001
8 vs. 1	-5917	-6969 to -4866	Yes	****	< 0.0001
10 vs. 1	-6358	-7409 to -5306	Yes	****	< 0.0001

Table S2

Statistics for **Fig. 3e**: 2-way ANOVA with factors of "Dilution Factor" and "Encapsulation".

Source of Variation	% of total variation	P value	P value summary	Significant?
Interaction	38.48	< 0.0001	****	Yes
Dilution Factor	50.55	< 0.0001	****	Yes
Encapsulation	1.665	0.0156	*	Yes

Dunnett's multiple comparisons test after the ANOVA.

	Mean Diff.	95% CI of diff.	Significant?	Summary	Adjusted P Value
Liposome					
2 vs. 1	-27.26	-177.3 to 122.8	No	ns	0.9854
4 vs. 1	-42.54	-192.6 to 107.5	No	ns	0.9129
6 vs. 1	-26.02	-176.1 to 124.1	No	ns	0.9881
8 vs. 1	-29.94	-180.0 to 120.1	No	ns	0.9781
10 vs. 1	-97.95	-248.0 to 52.13	No	ns	0.31
Solution					
2 vs. 1	-385.3	-535.4 to -235.2	Yes	****	< 0.0001
4 vs. 1	-582.8	-732.9 to -432.8	Yes	****	< 0.0001
6 vs. 1	-753.1	-903.2 to -603.0	Yes	****	< 0.0001
8 vs. 1	-827.7	-977.7 to -677.6	Yes	****	< 0.0001
10 vs. 1	-878.8	-1029 to -728.7	Yes	****	< 0.0001

Table S3

Statistics for **Fig. 3f**: 2-way ANOVA with factors of "Dilution Factor" and "Encapsulation".

Source of Variation	% of total variation	P value	P value summary	Significant?
Interaction	25.06	< 0.0001	****	Yes
Dilution Factor	34.95	< 0.0001	****	Yes
Encapsulation	33.06	< 0.0001	****	Yes

Dunnett's multiple comparisons test after the ANOVA.

	Mean Diff.	95% CI of diff.	Significant?	Summary	Adjusted P Value
Liposome					
2 vs. 1	15.96	-54.75 to 86.66	No	ns	0.9637
4 vs. 1	0.3899	-70.32 to 71.10	No	ns	> 0.9999
6 vs. 1	-14.33	-85.03 to 56.38	No	ns	0.9767
8 vs. 1	-22.41	-93.11 to 48.30	No	ns	0.8716
10 vs. 1	-44.25	-115.0 to 26.45	No	ns	0.3474
Solution					
2 vs. 1	-228.6	-299.3 to -157.9	Yes	****	< 0.0001
4 vs. 1	-314.7	-385.4 to -244.0	Yes	****	< 0.0001
6 vs. 1	-345.7	-416.4 to -275.0	Yes	****	< 0.0001
8 vs. 1	-382.9	-453.6 to -312.2	Yes	****	< 0.0001
10 vs. 1	-394.8	-465.5 to -324.0	Yes	****	< 0.0001

Table S4

Statistics for **Figs. 3j – 3l**: 3-way ANOVA with factors of “Time”, "Encapsulation" and "Order".

Source	Nparm	DF	Sum of Squares	F Ratio	Prob > F
Time	1	1	3612860	3.7024	0.061
Encapsulation	1	1	20048169	20.5452	<.0001
Order	2	2	218970231	112.1994	<.0001

Table S5

Statistics for **Fig. 3j**: 2-way ANOVA with factors of "Time" and "Encapsulation".

Source of Variation	% of total variation	P value	P value summary	Significant?
Interaction	1.308	0.2853	ns	No
Time	13.82	0.0034	**	Yes
Encapsulation	72.32	< 0.0001	****	Yes

Sidak's multiple comparisons test after the ANOVA

	Mean Diff.	95% CI of diff.	Significant?	Summary	Adjusted P Value
Solution - Liposome					
1h	2959	1474 to 4444	Yes	***	0.0005
3h	3879	2394 to 5364	Yes	****	< 0.0001

Table S6

Statistics for **Fig. 3k**: 2-way ANOVA with factors of "Time" and "Encapsulation".

Source of Variation	% of total variation	P value	P value summary	Significant?
Interaction	0.7342	0.5091	ns	No
Time	4.334	0.1241	ns	No
Encapsulation	75.91	< 0.0001	****	Yes

Sidak's multiple comparisons test after the ANOVA

	Mean Diff.	95% CI of diff.	Significant?	Summary	Adjusted P Value
Solution - Liposome					
1h	453.5	238.1 to 669.0	Yes	***	0.0003
3h	372.3	156.9 to 587.8	Yes	**	0.0017

Table S7

Statistics for **Fig. 3l**: 2-way ANOVA with factors of "Time" and "Encapsulation".

Source of Variation	% of total variation	P value	P value summary	Significant?
Interaction	4.032	0.4007	ns	No
Time	18.41	0.0872	ns	No
Encapsulation	13.84	0.1324	ns	No

Sidak's multiple comparisons test after the ANOVA

	Mean Diff.	95% CI of diff.	Significant?	Summary	Adjusted P Value
Solution - Liposome					
1h	70.26	-31.80 to 172.3	No	ns	0.1977
3h	21	-81.06 to 123.1	No	ns	0.8471

Table S8

Statistics for **Fig. 4b**: 2-way ANOVA with factors of "firefly or Renilla" and "alpha-Hemolysin Combination".

Source of Variation	% of total variation	P value	P value summary	Significant?
Interaction	34.06	< 0.0001	****	Yes
alpha-Hemolysin Combination	43.87	< 0.0001	****	Yes
firefly or Renilla	18.41	< 0.0001	****	Yes

Sidak's multiple comparisons test after the ANOVA. The four combinations of alpha-hemolysin (aHL) compared in this table correspond to the four clusters (of two bars each) in **Fig. 4b**. The concentrations of aHL DNA used to construct each liposome population are as follows:

aHL combination	aHL in firefly Luciferase liposomes	aHL in Renilla Luciferase liposomes
A	0.1 nM	0.1 nM
B	5 nM	5 nM
C	0.1 nM	5 nM
D	5 nM	0.1 nM

	Mean Diff.	95% CI of diff.	Significant?	Summary	Adjusted P Value
Firefly luciferase expression					
B vs. A	4730	2699 to 6761	Yes	****	< 0.0001
C vs. A	-80.77	-2112 to 1951	No	ns	> 0.9999
D vs. A	3498	1466 to 5529	Yes	***	0.0003
C vs. B	-4811	-6842 to -2780	Yes	****	< 0.0001
D vs. B	-1233	-3264 to 798.7	No	ns	0.45
D vs. C	3578	1547 to 5610	Yes	***	0.0002

Renilla luciferase expression					
B vs. A	10890	8859 to 12921	Yes	****	< 0.0001
C vs. A	9855	7824 to 11886	Yes	****	< 0.0001
D vs. A	-246.6	-2278 to 1785	No	ns	0.9996
C vs. B	-1035	-3066 to 996.4	No	ns	0.6416
D vs. B	-11137	-13168 to -9105	Yes	****	< 0.0001
D vs. C	-10102	-12133 to -8070	Yes	****	< 0.0001

Table S9

Statistics for **Fig. S13b**: 2-way ANOVA with factors of "Theophylline" and "Time".

Source of Variation	% of total variation	P value	P value summary	Significant?
Interaction	8.412	< 0.0001	****	Yes
Time	44.57	< 0.0001	****	Yes
Theophylline	45.6	< 0.0001	****	Yes

Sidak's multiple comparisons test after the ANOVA

	Mean Diff.	95% CI of diff.	Significant?	Summary	Adjusted P Value
+ Theo					
1 vs. 0	226.3	138.7 to 313.9	Yes	****	< 0.0001
2 vs. 0	425.5	337.9 to 513.1	Yes	****	< 0.0001
3 vs. 0	571	483.4 to 658.6	Yes	****	< 0.0001
4 vs. 0	661.8	574.2 to 749.4	Yes	****	< 0.0001
5 vs. 0	693.7	606.1 to 781.3	Yes	****	< 0.0001
6 vs. 0	774.6	687.0 to 862.2	Yes	****	< 0.0001
7 vs. 0	872.3	784.7 to 959.9	Yes	****	< 0.0001
8 vs. 0	889	801.4 to 976.6	Yes	****	< 0.0001
9 vs. 0	953.3	865.7 to 1041	Yes	****	< 0.0001
10 vs. 0	963.8	876.2 to 1051	Yes	****	< 0.0001
- Theo					
1 vs. 0	55.64	-31.96 to 143.2	No	ns	0.5177
2 vs. 0	109.1	21.53 to 196.7	Yes	**	0.0059
3 vs. 0	181.2	93.57 to 268.8	Yes	****	< 0.0001
4 vs. 0	217	129.4 to 304.6	Yes	****	< 0.0001
5 vs. 0	256.2	168.6 to 343.8	Yes	****	< 0.0001
6 vs. 0	294.4	206.8 to 382.0	Yes	****	< 0.0001
7 vs. 0	309.6	222.0 to 397.2	Yes	****	< 0.0001
8 vs. 0	337.4	249.8 to 425.0	Yes	****	< 0.0001
9 vs. 0	345.4	257.8 to 433.0	Yes	****	< 0.0001
10 vs. 0	368.8	281.2 to 456.4	Yes	****	< 0.0001

Table S10

Statistics for **Fig. S13d**: 2-way ANOVA with factors of "Arabinose" and "Time".

Source of Variation	% of total variation	P value	P value summary	Significant?
Interaction	17.39	< 0.0001	****	Yes
Time	17.5	< 0.0001	****	Yes
Arabinose	63.1	< 0.0001	****	Yes

Sidak's multiple comparisons test after the ANOVA

	Mean Diff.	95% CI of diff.	Significant?	Summary	Adjusted P Value
+ Ara					
1 vs. 0	253.7	-99.71 to 607.1	No	ns	0.3454
2 vs. 0	675.2	321.8 to 1029	Yes	****	< 0.0001
3 vs. 0	1332	978.8 to 1686	Yes	****	< 0.0001
4 vs. 0	1838	1484 to 2191	Yes	****	< 0.0001
5 vs. 0	2117	1764 to 2471	Yes	****	< 0.0001
6 vs. 0	2232	1879 to 2586	Yes	****	< 0.0001
7 vs. 0	2261	1908 to 2615	Yes	****	< 0.0001
8 vs. 0	2344	1991 to 2698	Yes	****	< 0.0001
9 vs. 0	2464	2110 to 2817	Yes	****	< 0.0001
10 vs. 0	2480	2126 to 2833	Yes	****	< 0.0001
- Ara					
1 vs. 0	0.5058	-352.9 to 353.9	No	ns	> 0.9999
2 vs. 0	1.534	-351.9 to 354.9	No	ns	> 0.9999
3 vs. 0	2.061	-351.4 to 355.5	No	ns	> 0.9999
4 vs. 0	2.881	-350.5 to 356.3	No	ns	> 0.9999
5 vs. 0	3.41	-350.0 to 356.8	No	ns	> 0.9999
6 vs. 0	2.614	-350.8 to 356.0	No	ns	> 0.9999
7 vs. 0	3.177	-350.2 to 356.6	No	ns	> 0.9999
8 vs. 0	3.376	-350.0 to 356.8	No	ns	> 0.9999
9 vs. 0	4.785	-348.6 to 358.2	No	ns	> 0.9999
10 vs. 0	4.89	-348.5 to 358.3	No	ns	> 0.9999

Table S11

Statistics for **Fig. 6**: 3-way ANOVA with factors of "Mechanism", "Occupancy A", "Occupancy B", and "SNARE compatibility". (i.e., whether the SNARE protein mimics are complementary, equal, or not present).

Source	Nparm	DF	Sum of Squares	F Ratio	Prob > F
Mechanism	4	4	1878842.8	6.1006	<.0001
Occupancy A	2	2	3944276.1	25.6142	<.0001
Occupancy B	2	2	4663508.3	30.2849	<.0001
SNARE Type	2	2	3745780.4	24.3251	<.0001

Literature

1. Crabb, D. W. & Dixon, J. E. A method for increasing the sensitivity of chloramphenicol acetyltransferase assays in extracts of transfected cultured cells. *Anal. Biochem.* **163,** 88–92 (1987).

2. Sun, Z. Z., Hayes, C. A., Shin, J., Caschera, F., Murray, R. M., Noireaux, V. Protocols for Implementing an *Escherichia coli* Based TX-TL Cell-Free Expression System for Synthetic Biology. *J. Vis. Exp.* (79), e50762, doi:10.3791/50762 (2013)

3. Stano, P. & Luisi, P. L. Semi-synthetic minimal cells: Origin and recent developments. *Curr. Opin. Biotechnol.* **24,** 633–638 (2013).

4. Agapakis, C. M. Designing Synthetic Biology. *ACS Synth. Biol.* **3,** 121–128 (2014).

5. Adamala, K. *et al.* Open questions in origin of life: experimental studies on the origin of nucleic acids and proteins with specific and functional sequences by a chemical synthetic biology approach. *Comput. Struct. Biotechnol. J.* **9,** e201402004 (2014).

6. Porcar, M. *et al.* The ten grand challenges of synthetic life. *Syst. Synth. Biol.* **5,** 1–9 (2011).

7. Naylor, L. H. Reporter gene technology: the future looks bright. *Biochem. Pharmacol.* **58,** 749–757 (1999).

8. Hakkila, K., Maksimow, M., Karp, M. & Virta, M. Reporter Genes lucFF, luxCDABE, gfp, and dsred Have Different Characteristics in Whole-Cell Bacterial Sensors. *Anal. Biochem.* **301,** 235–242 (2002).

9. Choy, G. *et al.* Comparison of noninvasive fluorescent and bioluminescent small animal optical imaging. *Biotechniques* **35,** 1022–1030 (2003).

10. Hall, M. P. *et al.* Engineered luciferase reporter from a deep sea shrimp utilizing a novel imidazopyrazinone substrate. *ACS Chem. Biol.* **7,** 1848–1857 (2012).

11. Lentini, R. *et al.* Integrating artificial with natural cells to translate chemical messages that direct E. coli behaviour. *Nat. Commun.* **5,** 4012 (2014).

12. Lentini, R. *et al.* Fluorescent Proteins and in Vitro Genetic Organization for Cell-Free Synthetic Biology. (2013).

13. Lewis, B. a & Engelman, D. M. Lipid bilayer thickness varies linearly with acyl chain length in fluid

phosphatidylcholine vesicles. *J. Mol. Biol.* **166,** 211–217 (1983).

14. Nezil, F. a. & Bloom, M. Combined influence of cholesterol and synthetic amphiphillic peptides upon bilayer thickness in model membranes. *Biophys. J.* **61,** 1176–1183 (1992).

15. Jousma, H. *et al.* Characterization of liposomes. The influence of extrusion of multilamellar vesicles through polycarbonate membranes on particle size, particle size distribution and number of bilayers. *Int. J. Pharm.* **35,** 263–274 (1987).

16. Olson, F., Hunt, C. a, Szoka, F. C., Vail, W. J. & Papahadjopoulos, D. Preparation of liposomes of defined size distribution by extrusion through polycarbonate membranes. *Biochim. Biophys. Acta* **557,** 9–23 (1979).

17. Berger, N., Sachse, a., Bender, J., Schubert, R. & Brandl, M. Filter extrusion of liposomes using different devices: Comparison of liposome size, encapsulation efficiency, and process characteristics. *Int. J. Pharm.* **223,** 55–68 (2001).

18. Caschera, F. & Noireaux, V. Compartmentalization of an all-E. coli Cell-Free Expression System for the Construction of a Minimal Cell. Artif. Life 22, 185-95 (2016).

19. Kamat, N. P. *et al.* Electrostatic Localization of RNA to Protocell Membranes by Cationic Hydrophobic Peptides. *Angew. Chemie - Int. Ed.* **54,** 11735–11739 (2015).

20. McAdams, H. H. & Arkin, a. Simulation of prokaryotic genetic circuits. *Annu. Rev. Biophys. Biomol. Struct.* **27,** 199–224 (1998).

21. Purnick, P. E. M. & Weiss, R. The second wave of synthetic biology: from modules to systems. *Nat. Rev. Mol. Cell Biol.* **10,** 410–422 (2009).

22. Shin, J. & Noireaux, V. An E. coli cell-free expression toolbox: Application to synthetic gene circuits and artificial cells. *ACS Synth. Biol.* **1,** 29–41 (2012).

23. Brödel, A. K. & Kubick, S. Developing cell-free protein synthesis systems: a focus on mammalian cells. *Pharm. Bioprocess.* **2,** 339–348 (2014).

24. Chang, H. C., Kaiser, C. M., Hartl, F. U. & Barral, J. M. De novo folding of GFP fusion proteins: High efficiency in eukaryotes but not in bacteria. *J. Mol. Biol.* **353,** 397–409 (2005).

25. Hillebrecht, J. R. & Chong, S. A comparative study of protein synthesis in in vitro systems: from the prokaryotic reconstituted to the eukaryotic extract-based. *BMC Biotechnol.* **8,** 58 (2008).

26. Sun, Z. Z. *et al.* Protocols for Implementing an Escherichia coli Based TX-TL Cell-Free Expression System for Synthetic Biology. *J. Vis. Exp.* 1–15 (2013). doi:10.3791/50762

27. Caschera, F. & Noireaux, V. A cost-effective polyphosphate-based metabolism fuels an all E. coli cell-free expression system. *Metab. Eng.* **27,** 29–37 (2015).

28. Garamella, J., Marshall, R., Rustad, M. & Noireaux, V. The all E. coli TX-TL Toolbox 2.0: a platform for cell-free synthetic biology. ACS Synth. Biol. 5, 3044-30445. acssynbio.5b00296 (2016). doi:10.1021/acssynbio.5b00296

29. Liu, D. V., Zawada, J. F. & Swartz, J. R. Streamlining Escherichia Coli S30 extract preparation for economical cell-free protein synthesis. *Biotechnol. Prog.* **21,** 460–465 (2005).

30. Kigawa, T. *et al.* Preparation of Escherichia coli cell extract for highly productive cell-free protein expression. *J Struct Funct Genomics* **5,** 63–68 (2004).

31. Machida, K., Masutan, M. & Imataka, H. Protein Synthesis in vitro: Cell-Free Systems Derived from Human Cells. (2012). doi:10.5772/48563

32. Mikami, S., Kobayashi, T., Masutani, M., Yokoyama, S. & Imataka, H. A human cell-derived in vitro coupled transcription/translation system optimized for production of recombinant proteins. *Protein Expr. Purif.* **62,** 190–198 (2008).

33. Xu, C., Hu, S. & Chen, X. Artificial cells: from basic science to applications. Mater. Today 00, 1-17. (2016).

34. Caschera, F. & Noireaux, V. Integration of biological parts toward the synthesis of a minimal cell. *Curr. Opin. Chem. Biol.* **22,** 85–91 (2014).

35. Mikami, S., Masutani, M., Sonenberg, N., Yokoyama, S. & Imataka, H. An efficient mammalian cell-free translation system supplemented with translation factors. *Protein Expr. Purif.* **46,** 348–57 (2006).

36. Chen, I. a. & Szostak, J. W. A Kinetic Study of the Growth of Fatty Acid Vesicles. *Biophys. J.* **87,** 988–998 (2004).

37. Chen, I. a., Salehi-Ashtiani, K. & Szostak, J. W. RNA catalysis in model protocell vesicles. *J. Am. Chem. Soc.* **127,** 13213–13219 (2005).